DOT/FAA-PS-88-16

Project Report
ATC-162

A Case Study of the 24 August 1986 FLOWS Microburst

M. A. Isaminger
P. J. Biron
R. G. Hallowell

28 November 1989

Lincoln Laboratory
MASSACHUSETTS INSTITUTE OF TECHNOLOGY
LEXINGTON, MASSACHUSETTS

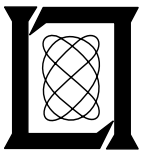

Prepared for the Federal Aviation Administration,
Washington, D.C. 20591

This document is available to the public through
the National Technical Information Service,
Springfield, VA 22161

TECHNICAL REPORT STANDARD TITLE PAGE

1. Report No.	2. Government Accession No.	3. Recipient's Catalog No.
DOT/FAA-PS-88-16		

4. Title and Subtitle	5. Report Date
A Case Study of the 24 August 1986 FLOWS Microburst	28 November 1989
	6. Performing Organization Code
7. Author(s)	8. Performing Organization Report No.
Mark A. Isaminger, Paul J. Biron, and Robert G. Hallowell	ATC-162
9. Performing Organization Name and Address	10. Work Unit No. (TRAIS)
Lincoln Laboratory, MIT P.O. Box 73 Lexington,MA 02173-9108	11. Contract or Grant No. DTFA-01-80-Y-10546
	13. Type of Report and Period Covered
12. Sponsoring Agency Name and Address Department of Transportation Federal Aviation Administration Program Engineering Service Washington, DC 20591	Project Report
	14. Sponsoring Agency Code

15. Supplementary Notes

This report is based on studies performed at Lincoln Laboratory, a center for research operated by Massachusetts Institute of Technology under Air Force Contract F19628-90-C-0002.

16. Abstract

From 1984 to 1986, Lincoln Laboratory under the sponsorship of the Federal Aviation Administration (FAA) collected wind shear measurements in the southeastern United States using a pulsed Doppler radar. The major emphasis of the measurement program and subsequent analyses is the development and testing of algorithms that will enable the Terminal Doppler Weather Radar (TDWR) to provide wind shear warnings to the aviation community by detection and tracking gust fronts and microbursts. An important phase of the program involves determining appropriate scan strategies and algorithms to detect other radar measurable features which precede or accompany the surface outflows of microbursts. The detection of features aloft such as convergence, rotation, divergence, storm cells, and descending reflectivity cores may permit advanced recognition of the wind shear while it is less than 10 m/s.

In this report a microburst on 24 August 1986 in Huntsville is analyzed with single and dual-Doppler techniques to assess microburst precursors, asymmetry, and forcing mechanisms which could be used for future algorithm development. The microburst producing storm formed within a moist adiabatic, unstable air-mass with weak wind shear at low to mid-levels of the atmosphere. Rotation, convergence, divergent tops, and a descending core were detected prior to the outflow attaining a divergenc of 10 m/s.

This storm is similar to other Huntsville microburst producing cells in exhibiting upper-level divergence prior to the initial microburst outflow. Previous analyses of wind shear in Denver and Oklahoma did not discuss divergent tops as a possible microburst precursor. However its relation to storm severity and hailstorm intensity has been reported by Witt and Nelson (1984) and NEXRAD Program Office (1985). In this case-study, the 3-dimensional microburst detection algorithm provided an early declaration of the event while the radial velocity differential was less than 10 m/s.

17. Key Words		18. Distribution Statement
TDWR	precursors	Document is available to the public through the National Technical Information Service, Springfield, VA 22161.
wind shear	asymmetry	
microburst	dual-Doppler	
features aloft	reflectivity notch	

19. Security Classif. (of this report)	20. Security Classif. (of this page)	21. No. of Pages	22. Price
Unclassified	Unclassified	88	

ABSTRACT

From 1984 to 1986, Lincoln Laboratory under the sponsorship of the Federal Aviation Administration (FAA) collected wind shear measurements in the southeastern United States using a pulsed Doppler radar. The major emphasis of the measurement program and subsequent analyses is the development and testing of algorithms that will enable the Terminal Doppler Weather Radar (TDWR) to provide wind shear warnings to the aviation community by detecting and tracking gust fronts and microbursts. An important phase of the program involves determining appropriate scan strategies and algorithms to detect other radar measurable features which precede or accompany the surface outflows of microbursts. The detection of features aloft such as convergence, rotation, divergence, storm cells, and descending reflectivity cores may permit advanced recognition of the wind shear while it is less than 10 m/s.

In this report a microburst on 24 August 1986 in Huntsville is analyzed with single and dual-Doppler techniques to assess microburst precursors, asymmetry, and forcing mechanisms which could be used for future algorithm development. The microburst producing storm formed within a moist adiabatic, unstable air-mass with weak wind shear at low to mid-levels of the atmosphere. Rotation, convergence, divergent tops, and a descending core were detected prior to the outflow attaining a divergence of 10 m/s.

This storm is similar to other Huntsville microburst producing cells in exhibiting upper-level divergence prior to the initial microburst outflow. Previous analyses of wind shear in Denver and Oklahoma did not discuss divergent tops as a possible microburst precursor. However its relation to storm severity and hailstorm intensity has been reported by Witt and Nelson (1984) and NEXRAD Program Office (1985). In this case-study, the 3-dimensional microburst detection algorithm provided an early declaration of the event while the radial velocity differential was less than 10 m/s.

ACKNOWLEDGEMENTS

The authors would like to thank Dr. Ron Rinehart for encouragement, editing, and drafting Figure IV-1. Constructive comments were supplied by Dr. Jim Evans, Mark Merritt, Marilyn Wolfson, and Dr. Steve Campbell. Software support from Ben Stevens and Rich Delaura helped produce the graphics. Thanks to Barbara Bennett for typing the manuscript. Warmest regards to Dr. John A. Sobol for support and encouragement. The radar data could not have been collected without the dedication of the FL-2 (Nat Fischer, Chuck Curtiss, and Stan Dajnak) and UND (Al Borho, Dave Bernhardt, Brad Assilen, Scott Kroeber, and Laurie Hermes) crews. Finally, thanks to our sponsors within the FAA, without whom this work would not be possible.

CONTENTS

LIST OF ILLUSTRATIONS

List of Tables

LIST OF ACRONYMS

AGL	Above Ground Level
ATC	Air-Traffic Control
CLAWS	Classify, Locate, and Avoid Wind Shear
dBz	Radar Reflectivity Factor
DFW	Dallas-Fort Worth International Airport
FAA	Federal Aviation Administration
FLOWS	FAA-Lincoln Laboratory Operational Weather Studies Project
FL-2	FAA-Lincoln Laboratory S-band Testbed Doppler Radar
JAWS	Joint Airport Weather Studies
LAWS	Low-Altitude Wind Shear
LLWAS	Low-Level Wind Shear Alert System
MESONET	Network of Automatic Weather Stations
MIST	Microbursts In Severe Thunderstorms
MSL	Mean Sea Level
NCAR	National Center For Atmospheric Research
NEXRAD	Next Generation Weather Radar
NIMROD	Northern Illinois Meteorological Research On Downbursts
NSSL	National Severe Storms Laboratory
PPI	Plan Position Indicator
RHI	Range Height Indicator
SKEWT	Upper-air Sounding
TDWR	Terminal Doppler Weather Radar
UND	University of North Dakota C-band Doppler Radar
UT	Universal Time

A Case-Study of the 24 August 1986 FLOWS Microburst

I. INTRODUCTION

From 1984 to 1986, Lincoln Laboratory under the sponsorship of the Federal Aviation Administration (FAA) collected measurements on low-level wind shear in the southeastern United States. The primary focus of the measurement program and subsequent analyses was the detection and warning of microburst wind shears in the airport terminal area. Previous research by Fujita (1981), Fujita and Wakimoto (1981), and McCarthy et al. (1982) alluded to the impact of microbursts on departing and arriving aircraft. Since 1964, a number of aviation accidents and incidents have been at least partially attributed to wind shear (National Research Council, 1983). The most recent, in Dallas, occurred during 1985 (Fujita, 1986 and Caracena et al., 1986). One goal of the Lincoln studies for the FAA is the development and testing of Terminal Doppler Weather Radar (TDWR) wind shear detection algorithms. The TDWR algorithm developed at Lincoln Laboratory (Campbell and Merritt, 1987 and Campbell, 1988) utilizes features aloft e.g., rotation, convergence, divergence, storm cells, and descending reflectivity cores as well as surface outflow features to detect microbursts.

The use of upper-altitude features (precursors) appears to provide improved microburst detection versus a surface outflow algorithm especially on weak (< 15 m/s) events and in some cases provides a more timely warning (Campbell, 1988). Aviation system users would like the reliable prediction of microbursts so that planes can plan their flight profiles to avoid microburst penetrations. This necessarily will require the use of precursors.

Another potential use of features aloft is to supplement warnings in the middle or later stages of an event in cases where the outflow increases after having weakened to near or below the hazard warning threshold (10 m/s). However, many details of precursors such as 1) location in space as a function of time in relation to the microburst life cycle, and 2) the probability of occurrence in microburst and non-microburst storms are not well understood. Gaining a better understanding of the precursor phenomena will assist in refining the TDWR scan strategy and microburst detection algorithm as well as leading to reliable predictions of microburst occurrence.

A radial velocity divergence of 10 m/s or greater at low levels over a distance of 4 km or less is generally regarded as a microburst (Wilson et al., 1984). An examination of the Huntsville data set documented several hundred outflows which attained this criteria. All radar detected microbursts during 1986 were classified as wet with reflectivities in excess of 35 dBz at the surface. On 24 August 1986, there were a number of microbursts detected to the west and northwest of the TDWR testbed in Huntsville, Alabama. In this report the strongest outflow is analyzed for possible precursors, asymmetry, and forcing mechanisms. The maximum reflectivity within the core was comparable to other southeastern United States microburst storms (Rinehart and Isaminger, 1986). The results of this study will be contrasted with microburst models derived from previous projects such as JAWS (Denver), CLAWS (Denver), and NSSL Spring Program (Oklahoma).

A. MEASUREMENT SYSTEM AND SPATIAL GEOMETRY

The primary sensor in the TDWR development program is the FAA testbed S-band Doppler radar (FL-2). This system utilizes a 1 degree pencil beam antenna and advanced signal processing capabilities to detect low-level wind shear. For more information on the hardware aspects of the system refer to Evans and Johnson, 1984. During the winter of 1985-86, the radar was assembled near the Huntsville-Madison County Airport (Figure I-1). The UND C-band Doppler radar was situated 15 km northwest of FL-2. For additional information on the UND system refer to Rinehart et al. (1987). The simultaneous measurements by two Doppler radars allows for a 2-dimensional analysis of the microburst surface wind field. This is important in determining the under or over-estimation of radial velocity based on a single radar and achieving a better understanding of the microburst generation process. Table I-1 summarizes the key technical characteristics of the FL-2 and UND radars for this research. Figure I-1 depicts the location of the radars and the microburst at maximum intensity. The dual-Doppler viewing angle from the microbursts center is approximately 40 degrees.

Table I-1 Characteristics Of Doppler Radars Used For This Study In Huntsville, Alabama

Characteristic	FL-2	UND
Beamwidth (deg)	1	1
Wavelength (cm)	10.6	5.4
Peak Power (kw)	1100	250
Sensitivity At Nominal Range Of 50 km (dBz)	-5.5	-3.1
Clutter Suppression (dB)	50	20
Maximum Range (km)	200	226
Range Gate Spacing (m)	120	250
Scan Strategy	PPI/RHI	PPI/RHI
Maximum Scan Rate (deg/sec)	10	16
Approximate Interval Between Surface Scans (min)	2	2
Approximate Volume Scan Time (min)	2	2
Elevation Angles To Scan Aloft	1 deg steps to 4 1.5 deg steps to 14.5	1 deg steps to 5 1.5 deg steps to 15.5

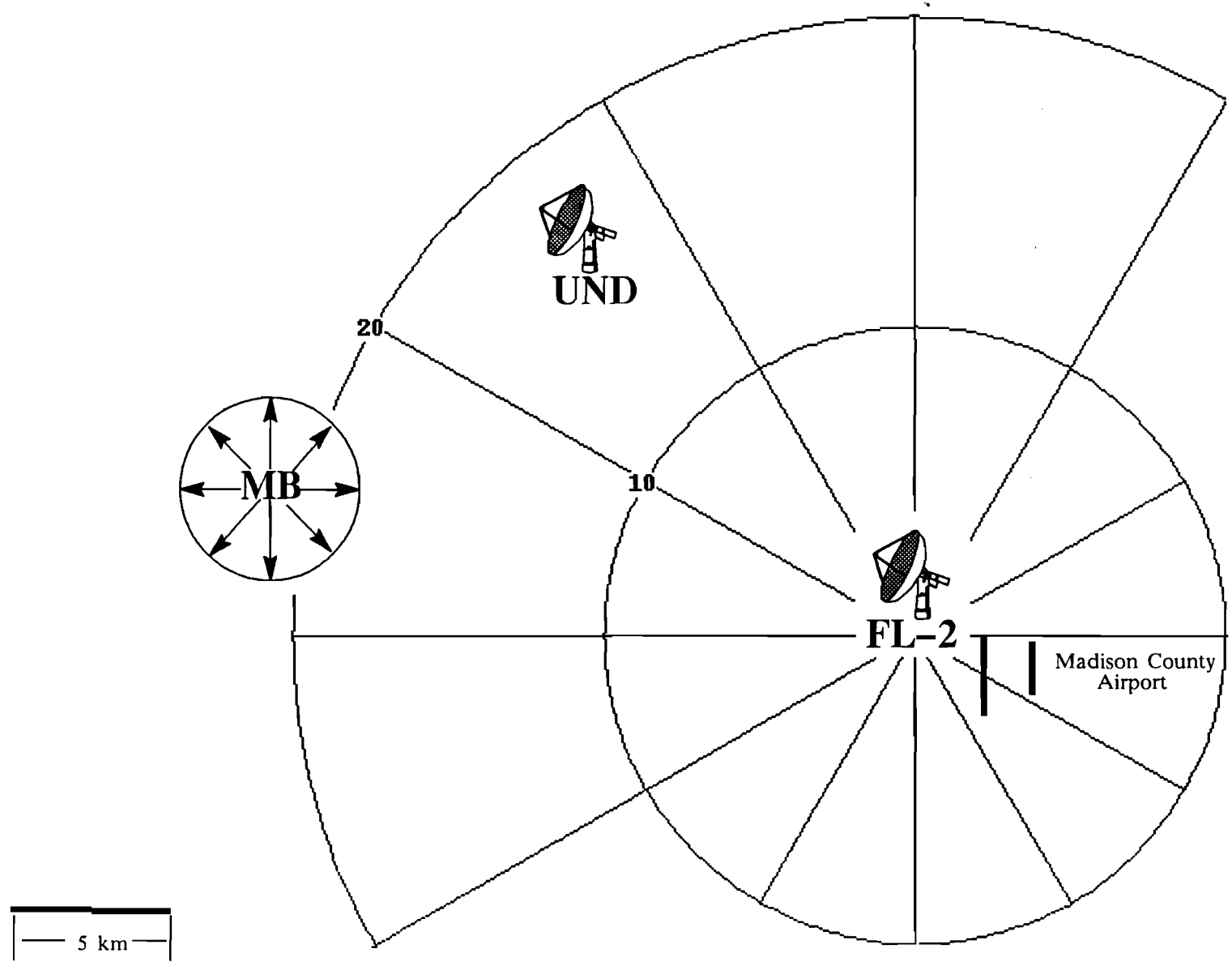

Figure I-1. Location of the 24 August 1986 Microburst in Relation to the UND and FL-2 Radars.

B. MICROBURST PRECURSORS

Previous researchers focused on the importance of forecasting or nowcasting (short-term forecast of 0 to 30 minutes) a microburst [Eilts (1987), Roberts and Wilson (1986), McCarthy and Wilson (1984), McCarthy et al. (1986), Wakimoto (1985), Roberts and Wilson (1984), and Caracena et al. (1983)]. During the CLAWS project at Denver, radar meteorologists from NCAR provided real time warnings of wind shears to ATC based on the detection of precursors and a weak surface divergence of < 10 m/s. Roberts and Wilson (1984) alluded to the fact that convergence aloft and a descending core were good indicators of a downdraft. Elmore (1986) and Roberts and Wilson (1986) associated reflectivity notching (*) with many microburst producing storms in the High Plains. In addition, numerous studies documented the presence of rotation during the microburst life cycle in the Denver area (Fujita and Wakimoto, 1981 and Kessinger et al., 1986). Collapsing storms is another feature that might be indicative of an outflow (Roberts and Wilson, 1986). Eilts (1987) reported the significance of a descending core and mid-level convergence in Oklahoma downbursts, while Fujita (1987) discussed a sinking top as a possible precursor to a microburst during MIST on 20 July 1986 in Huntsville, Alabama.

In this report we will investigate a microburst on 24 August 1986 in Huntsville, Alabama to determine the presence and temporal relationship of the precursors presented above as well as upper-level divergence (divergent tops). Divergent tops are a possible indicator of storm severity due to large hail (Witt and Nelson, 1984) and strong updrafts (NEXRAD Program Office, 1985). A previous study by Isaminger (1987) reported that upper-level divergence was detected in over 90% of the Huntsville microburst cases which were scanned to storm top. Its importance is magnified when considering none of the non-microburst cases exhibited divergent storm tops. Upper-altitude features have been included in the current version of the microburst detection algorithm (Campbell and Merritt, 1987 and Campbell, 1988). The algorithm utilizes features aloft to improve performance by declaring a microburst when the surface divergence is > 7.5 m/s and a precursor is detected. The 7.5 m/s threshold is a site adaptable parameter which may be adjusted as further experiments and analyses are carried out. Detailed time history studies such as described here are essential for determining the extent to which accurate (e.g., in time of occurrence and severity) microburst predictions can be achieved as well as in arriving at appropriate scan strategies. Among the precursors observed in this study are a descending core, divergence aloft, rotation, convergence, and reflectivity notching.

Each precursor will now be defined in the context used in this report. Velocity features were distinguished by a radial velocity difference (divergence and convergence) or an azimuthal velocity change (rotation) of 10 m/s. Convergence and rotation at altitudes between 1 and 7 km were considered mid-level precursors, while divergent tops are an upper-level feature (altitude > 7 km). In addition, divergences between the lowest elevation tilt and 1 km AGL were termed lower-level divergence. The spatial scale of features aloft for this storm was similar to the typical microburst.

(*) A reflectivity notch is distinguished by a region of lower reflectivity surrounded by higher reflectivity within a storm cell.

Storm cells were defined as the region enclosed by the 30 dBz contour. Reflectivity cores were characterized by the following criteria: 1) a maximum reflectivity of 50 dBz or greater, 2) the maximum reflectivity must develop at a height of > 2.5 km AGL, and 3) the depth of the 50 dBz reflectivity region must exceed 5.2 km (Isaminger, 1987). Descending cores were declared whenever the bottom of the 50 dBz contour dropped below 2 km. The thresholds presented in this study should not be regarded as definitive precursor values since it is possible that these thresholds will be modified once the microburst phenomena is better understood.

II. ATMOSPHERIC CONDITION

Figure II-1 is a upper-air sounding (SKEWT) from Nashville, Tennessee, at 1200 UT (0700 LDT) on 24 August 1986. There is abundant moisture between the surface and mid-levels with a wedge of drier air evident at 3.5 and 6 km AGL. The freezing layer is at a height of 4.6 km This is distinctly different from the dry adiabatic sounding conducive to High Plains microbursts (Wakimoto, 1985). In a study of Oklahoma downbursts, Eilts (1987) presented a sounding similar to Figure II-1. The air-mass in the region was unstable with a lifted index of -2. Weak wind shear conditions prevailed at low to mid-levels of the atmosphere. The surface winds were northwesterly at < 10 knots. By 1900 UT, the average mesonet temperature had exceeded 32 C with a dewpoint of 22 C. This was a typical hot and humid summer day in the southeastern United States.

Caracena et al. (1983) in an examination of JAWS soundings reported a high probability for microbursts if the 700-500 mb lapse rate is 8 degrees C/km or greater. The 850-700 mb lapse rate for this case-study was calculated as 7.5 degrees C/km from the Nashville sounding. Due to elevation differences the atmosphere between 850 and 700 mb in a moist sub-cloud environment (Huntsville) is similar to the 700-500 mb level at Denver. The relation of dry air at mid-levels, a moist sub-cloud layer, and a steep lapse rate in possible microburst forcing mechanisms will be discussed later.

III. EVENT ANALYSIS

By 1800 UT, several echoes were developing aloft west and northwest of FL-2. Some produced weak outflows while others did not. The microburst-producing storm formed at 1830 UT within a cluster of three echoes and lasted approximately 1 hour. It drifted southeastward with the prevailing winds at 15 km/hr.

A. 184854 UT FEATURES

Figure III-1 is an RHI which depicts two developing echoes at 184854 UT. The microburst-producing cell is farthest from the radar. For this and subsequent single-Doppler RHI analyses the FL-2 radar is located in the lower left corner of the plot. The storm tops are 8.4 km with a maximum surface reflectivity of 35 dBz. Several reflectivity regions > 50 dBz are detectable aloft between 1.5 and 5 km.

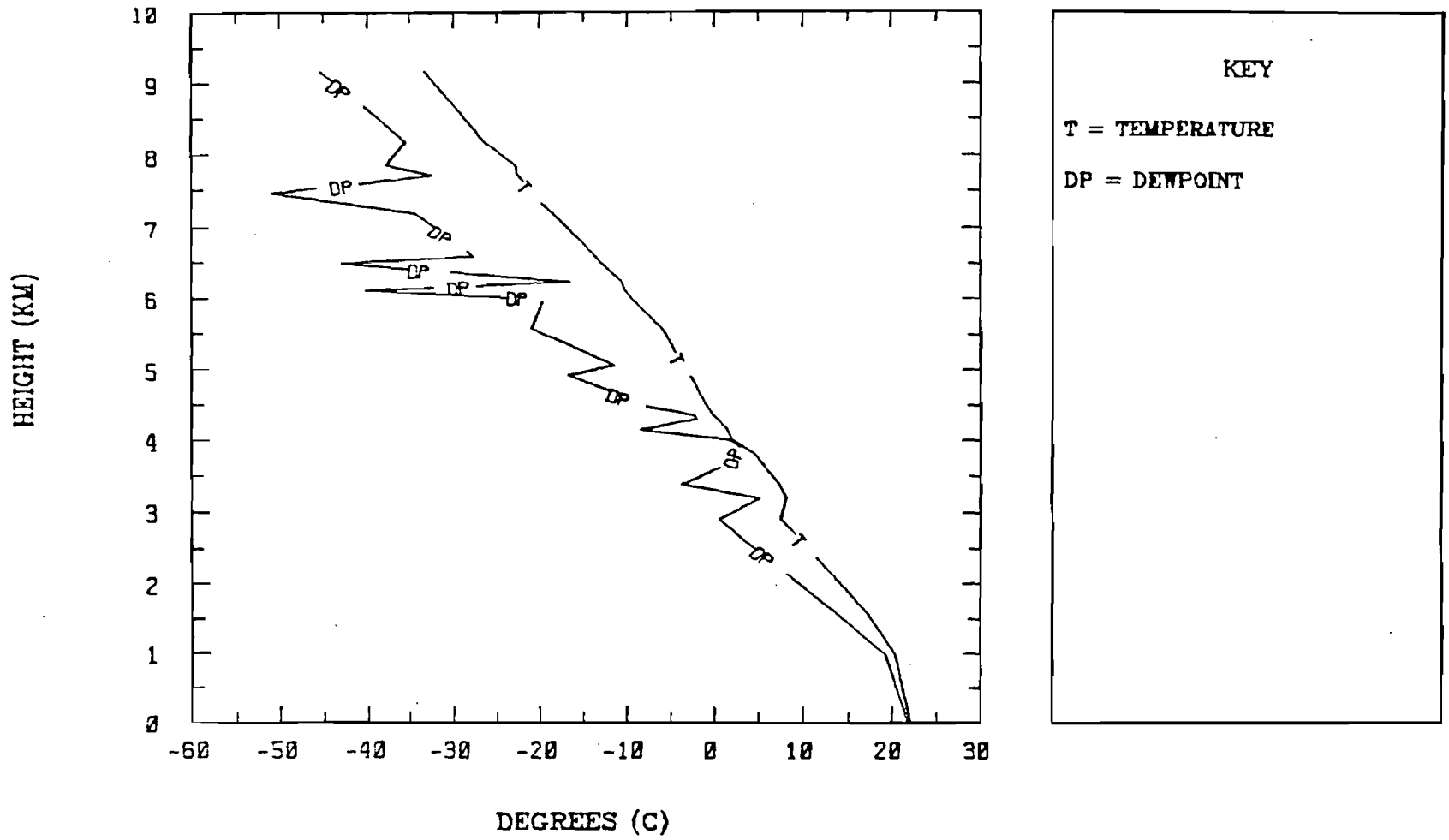

Figure II-1. Nashville Sounding - 24 August 1986 (122 UTC).

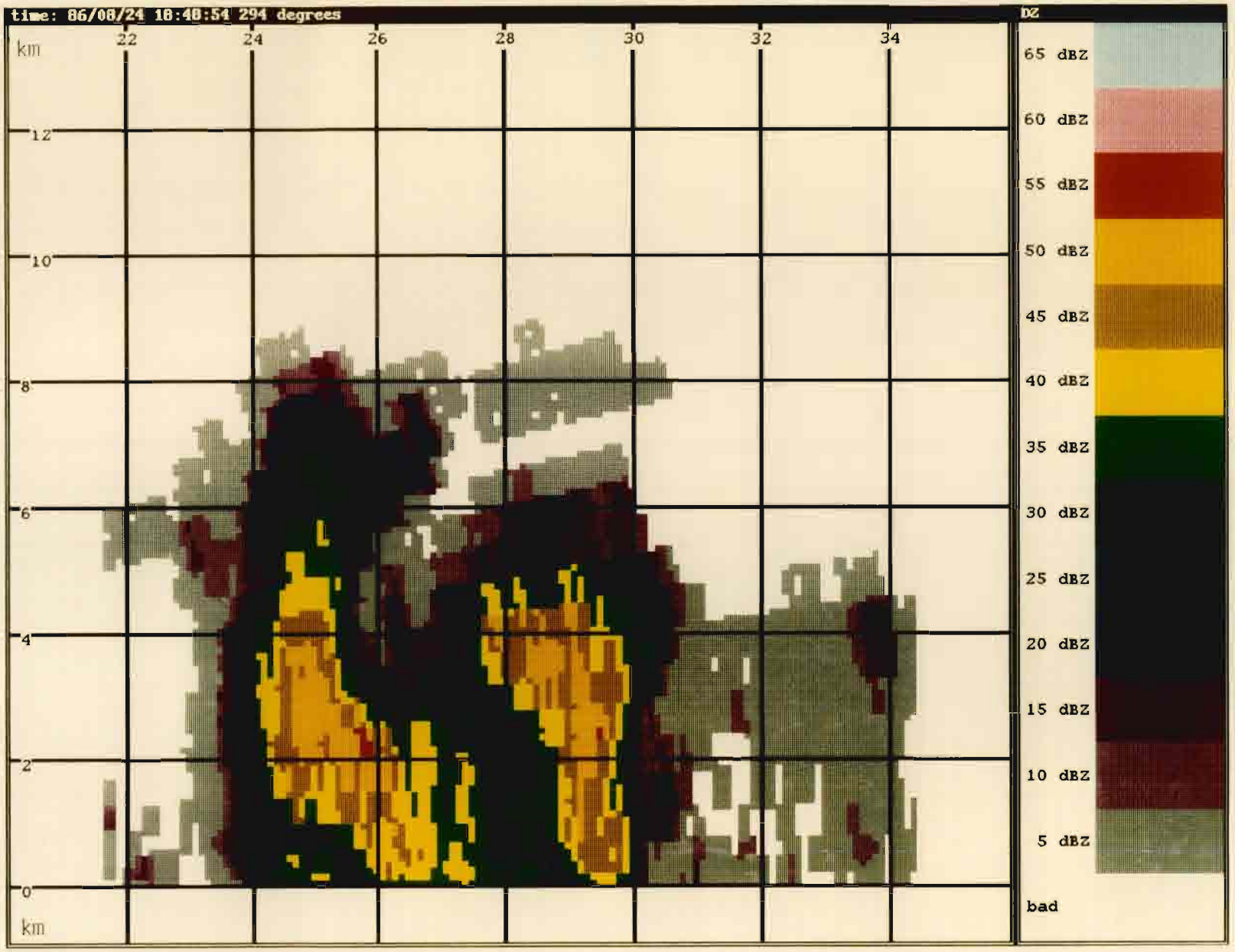

Figure III-1. RHI plot of Reflectivity Factor (184854 UTC)

B. 185659 UT FEATURES

Over an 8-minute period the height of the echo has expanded 2.6 km (Figure III-2). The area within the 50 dBz contour has increased and descended closer to the surface. This is the first indication of a reflectivity core since the depth of the 50 dBz echo exceeds 5.2 km.

C. 190052 UT FEATURES

In Figure III-3, a divergent top (A) at 9 km AGL and convergence (B) at the surface are indicative of a strong updraft. By 190052, the cloud tops have grown to 11.7 km (Figure III-4). The core has almost tripled in area with a maximum reflectivity of 60 dBz. In addition, the 40 dBz echo has extended to 9.1 km in altitude.

D. 190455 UT FEATURES

By 190455, upper-level divergence (A) of 24 m/s is apparent at 12-14 km AGL (Figure III-5). The surface outflow at this time is < 10 m/s. A second updraft is located by the divergence at B. The storm top has increased to 14.5 km and the core has fallen (Figure III-6). Another reflectivity maxima is noted at a height of 4 km AGL.

E. 190532 UT FEATURES

Figure III-7 is a dual-Doppler plot of horizontal winds in the lowest 500 meters. The raw wind field has been smoothed by a 9-point median filter to reduce the effects of noise (*). There is weak divergence (A) centered at -24 km East and 7.5 km North of FL-2. The mean surface winds from the northwest accounts for the stronger outflow to the southeast. This pattern has been noted by JAWS researchers such as Hjelmfelt (1987) and Kessinger et al. (1983). The smoothed divergence is 12.5 x 10-3 s-1, with a maximum radial velocity differential of 9 m/s A PPI at 190632 displays a rotational couplet (A) at 24 km and 290 deg (Figure III-8). A reflectivity notch (A) is apparent at a height of 3.4 km (Figure III-9). Both features (rotation and reflectivity notch) were detected within the cloud from 2 to 5 km AGL.

F. 190858 UT FEATURES

At 190858, an elongated protuberance termed a "flare" (A) is detected on the backside of the core at a height of 3.5 to 7.4 km (Figure III-10). For more information on this anomaly refer to Wilson and Reum (1987), Zrnic (1987), and Fujita (1987). The storm top has become partially detached at a height of 9 km. By 190914 (Figure III-11), the core extends from near the surface to a height of 6.7 km AGL. In addition, the top of the echo has fallen since the 190455 analysis. This could be representative of a sinking top as discussed by Fujita (1987) in an examination of the Monrovia Microburst on 20 July 1986 in Huntsville, Alabama. In Figure III-12, there is weak convergence (A) at a height of 3 km AGL.

(*) The filtering algorithm requires that at least 4 of the 9 data points contain valid data to be included in the final wind field.

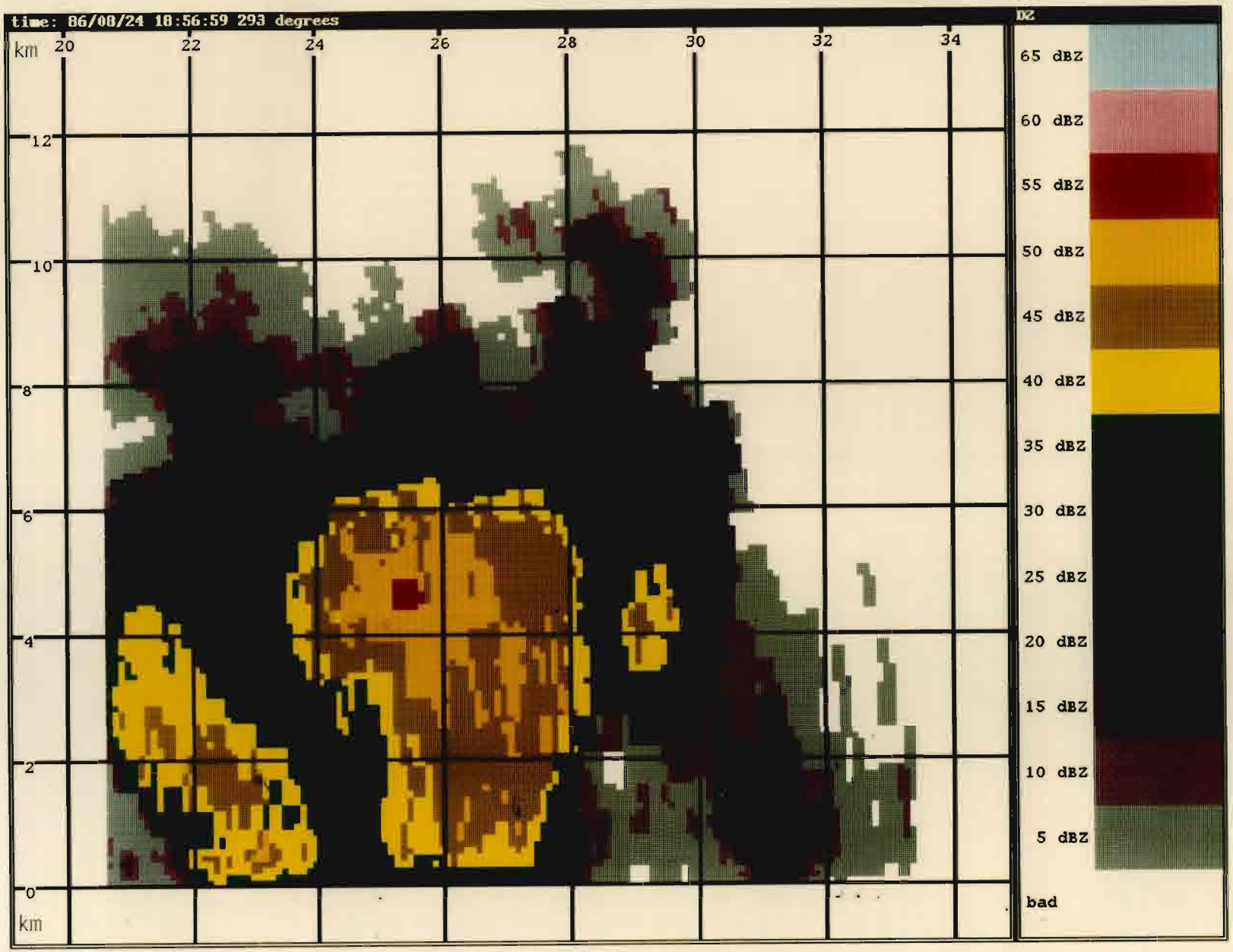

Figure III-2. RHI plot of Reflectivity Factor (185659 UTC)

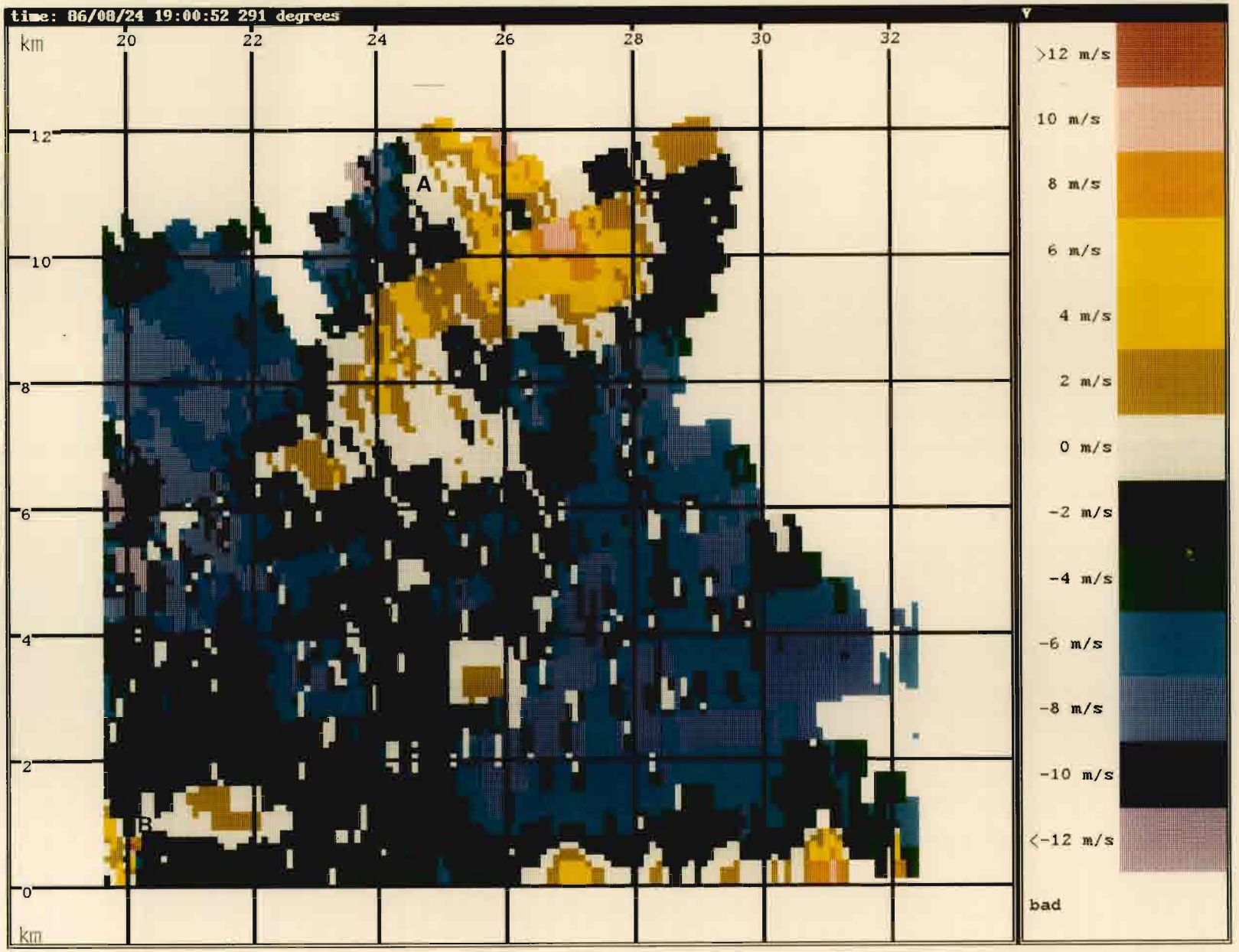

Figure III-3. RHI plot of Doppler Velocity (190052 UTC)

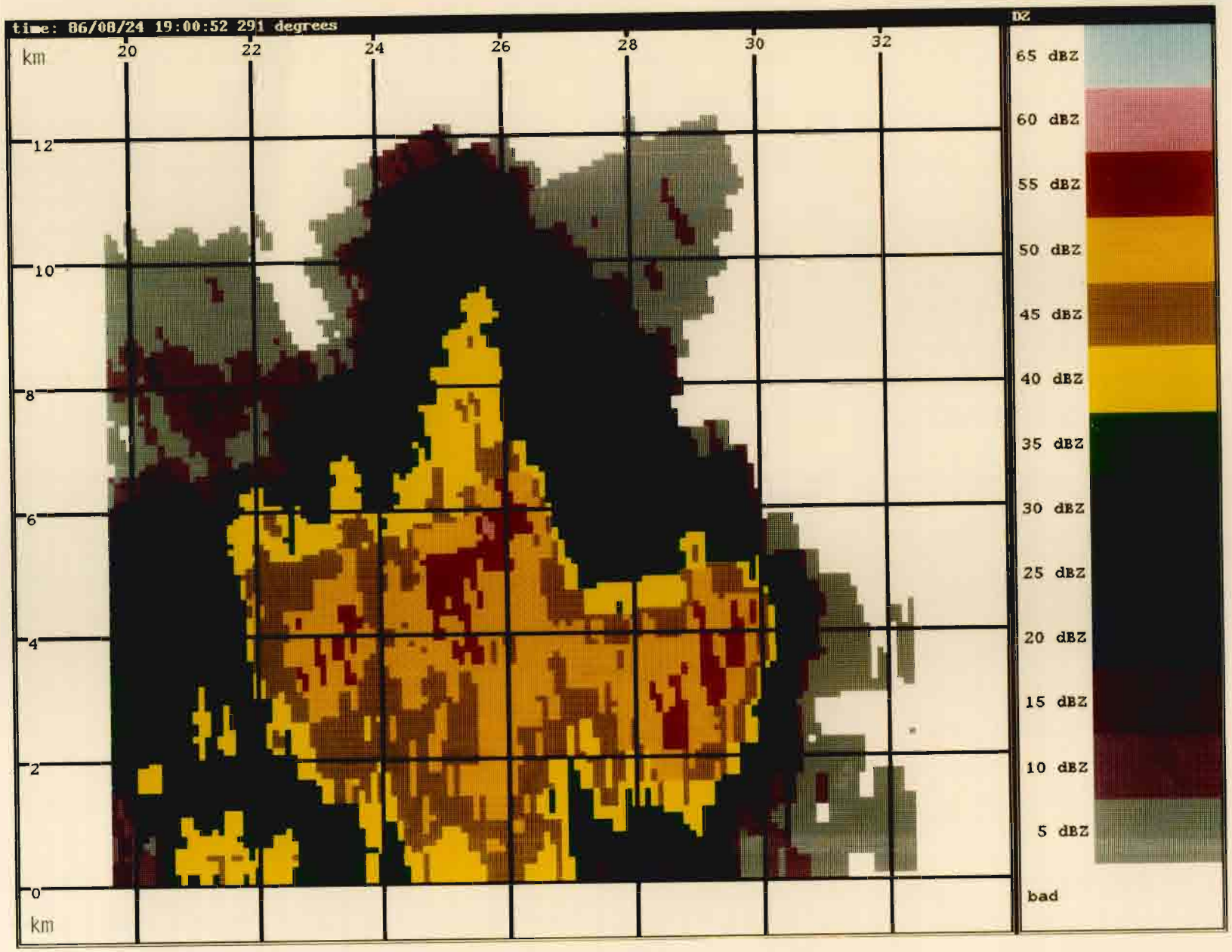

Figure III-4. RHI plot of Reflectivity Factor (190052 UTC)

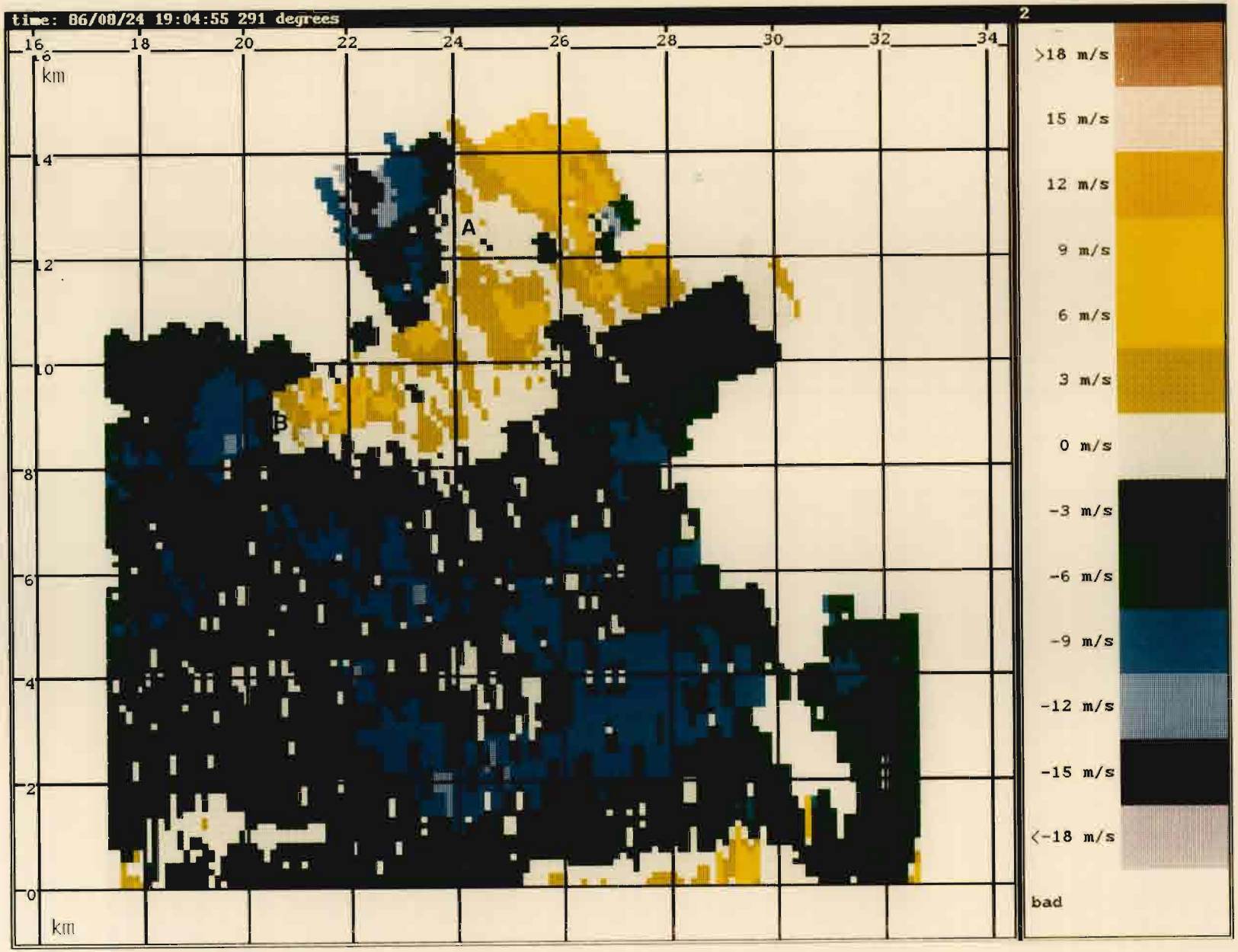

Figure III-5. RHI plot of Doppler Velocity (190455 UTC)

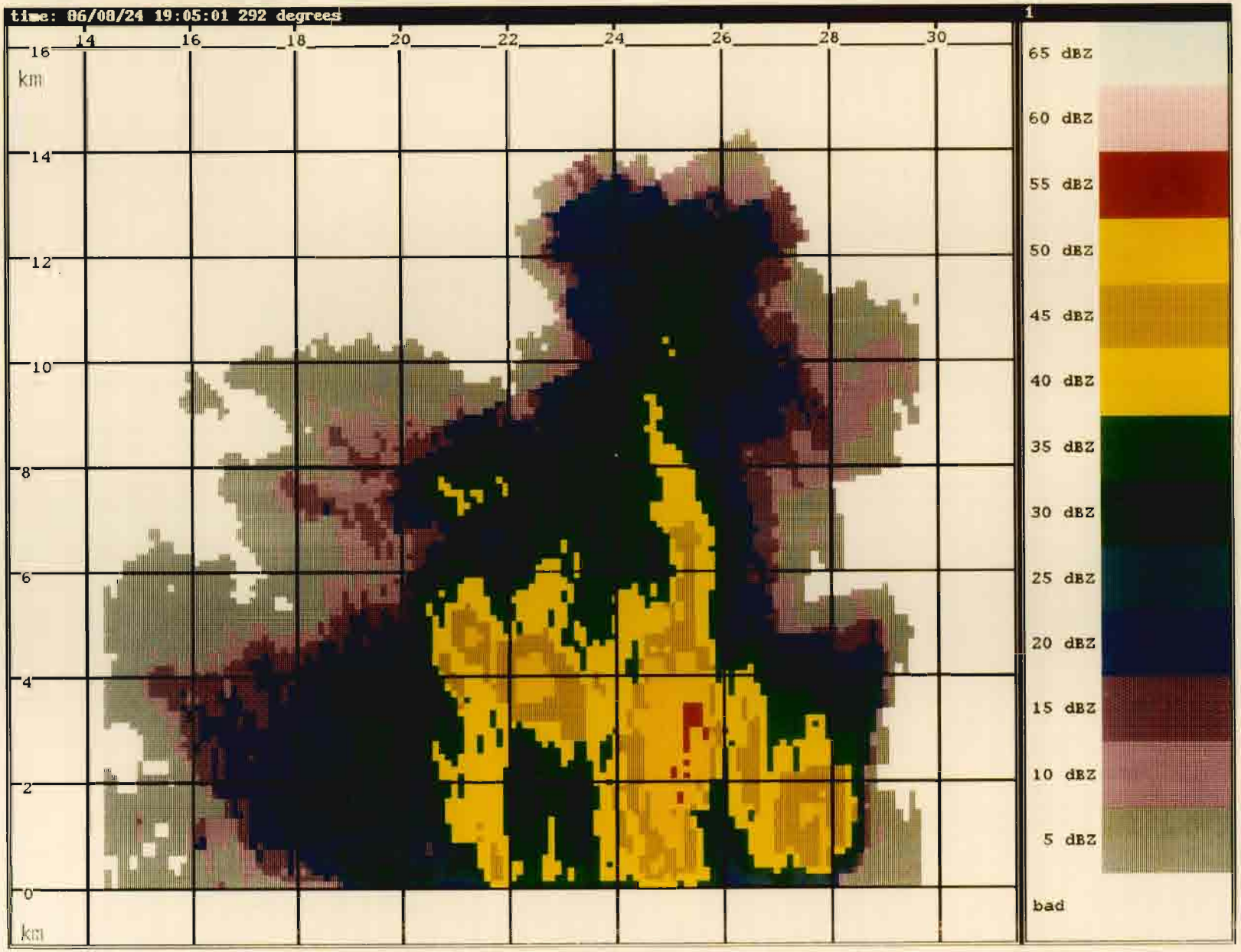

Figure III-6. RHI plot of Reflectivity Factor (190501 UTC)

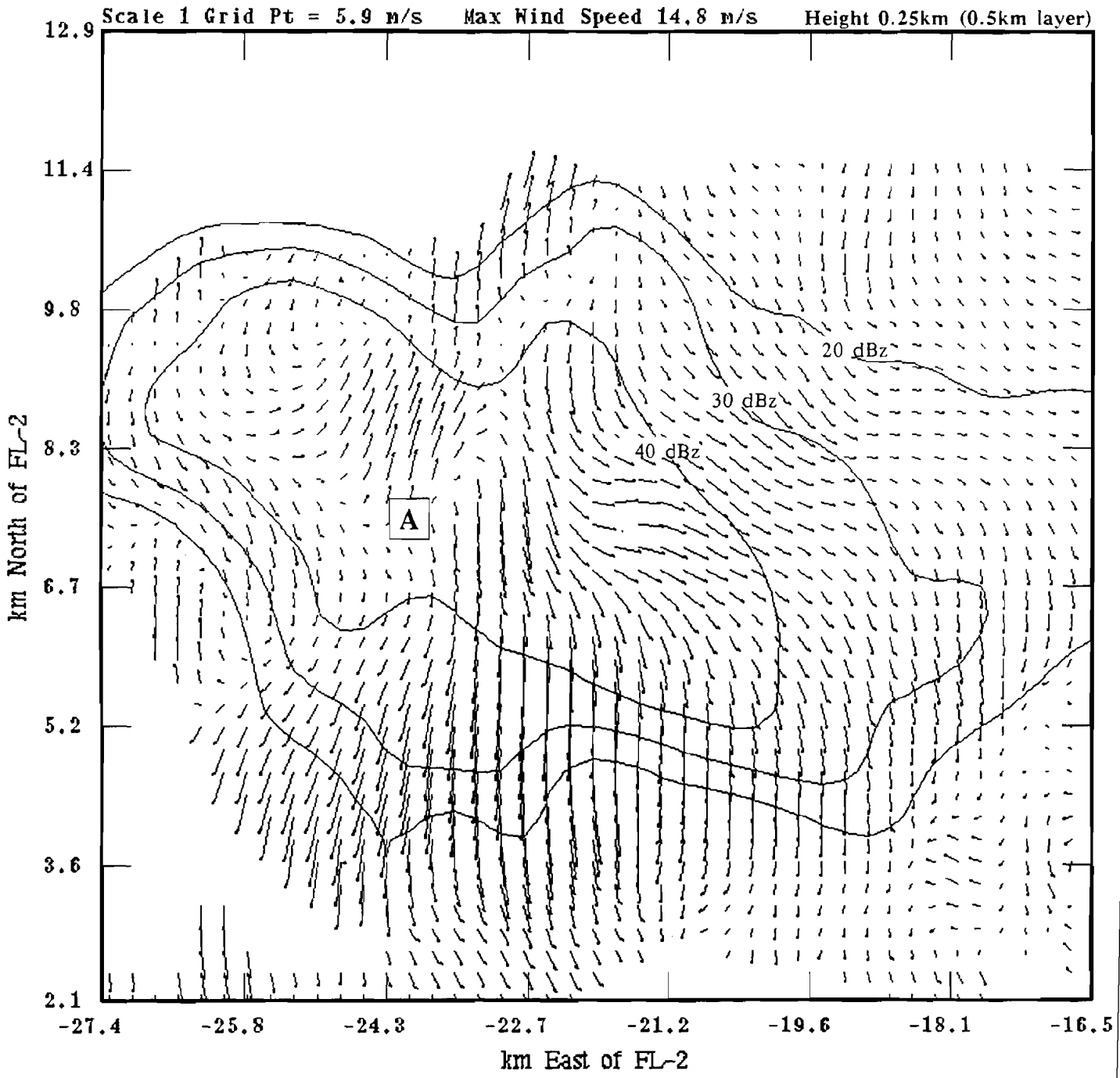

Figure III-7. Dual-Doppler Wind and dBz Plot (190532 UTC).

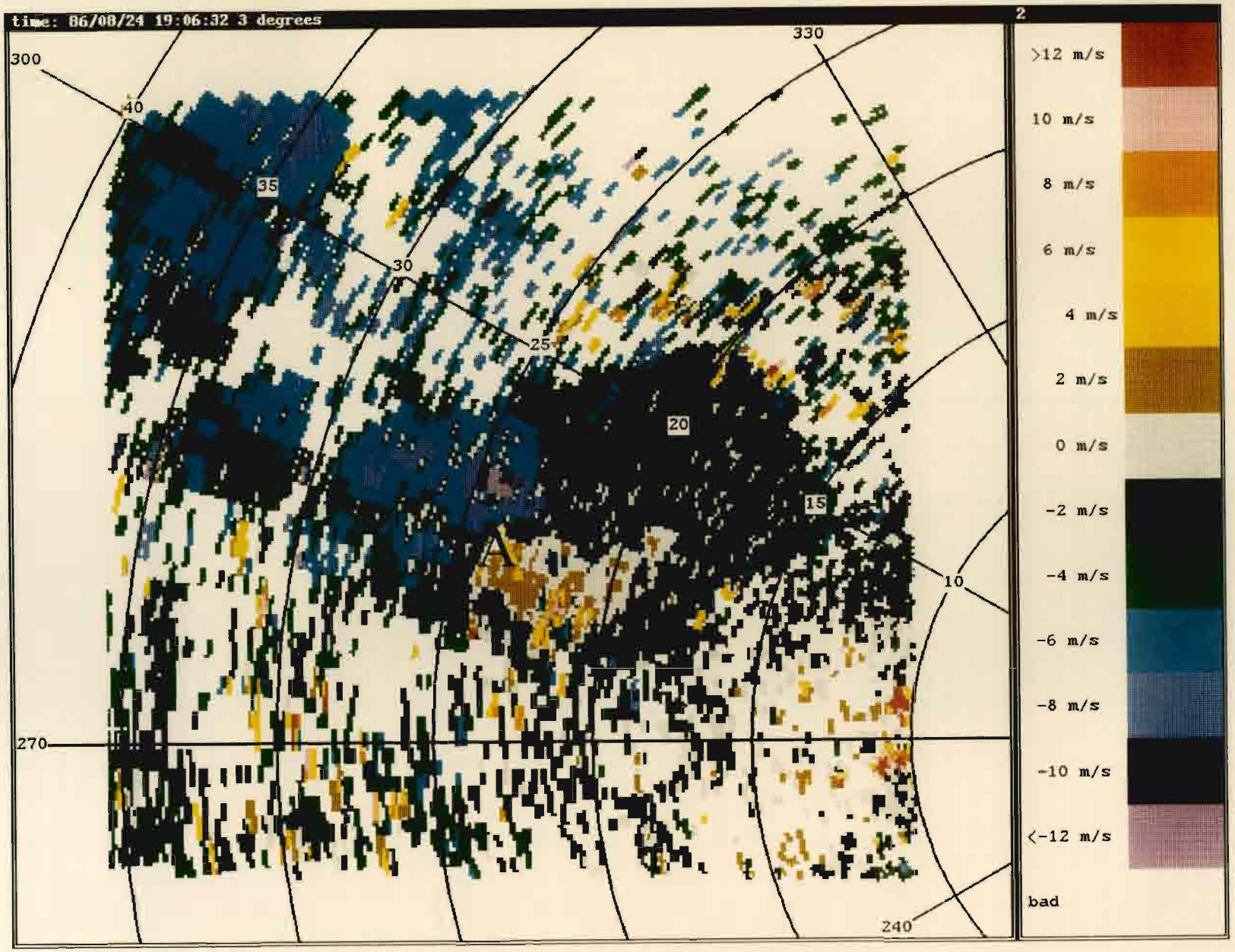

Figure III-8. PPI plot of Doppler Velocity (190632 UTC)

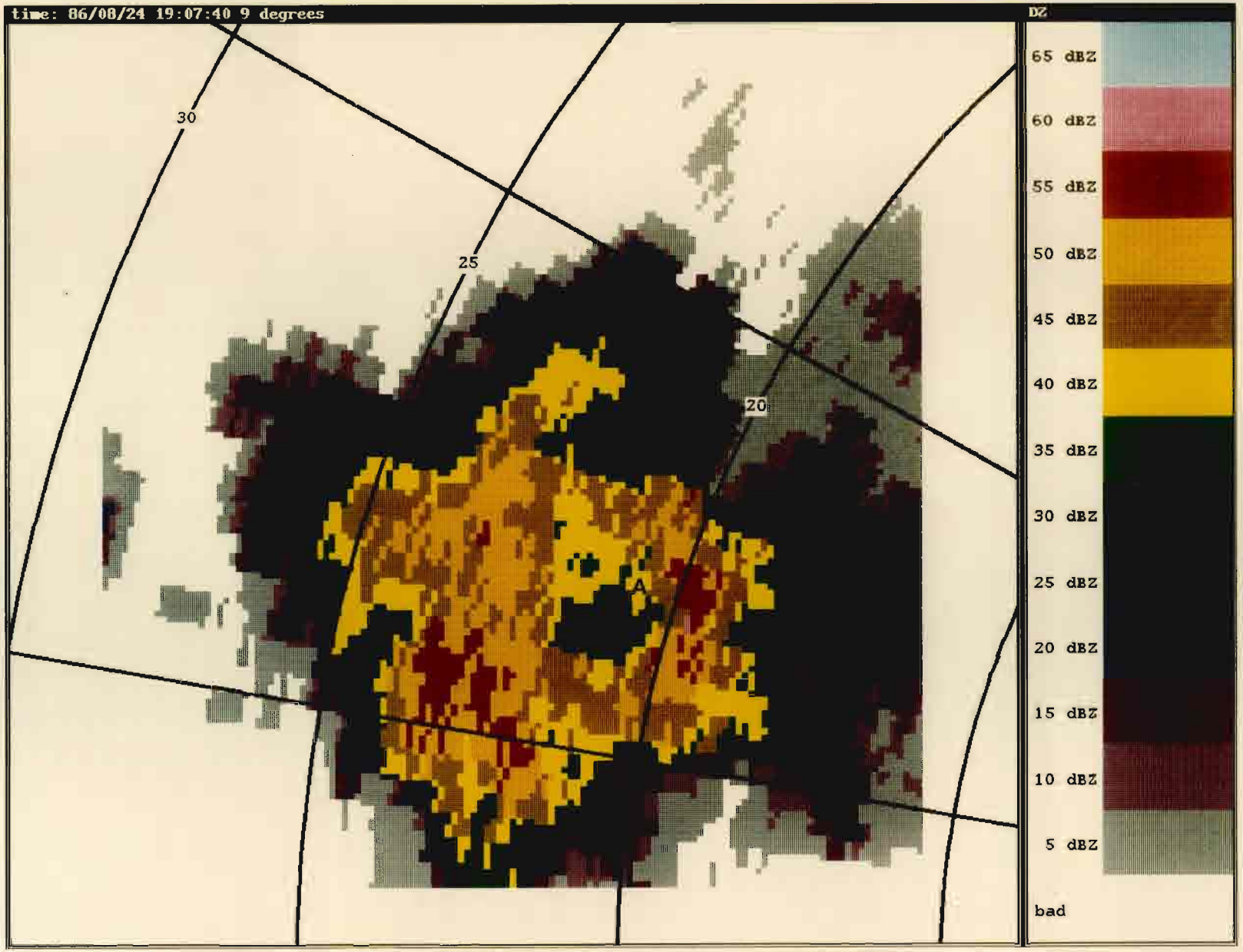

Figure III-9. PPI plot Reflectivity Factor (190740 UTC)

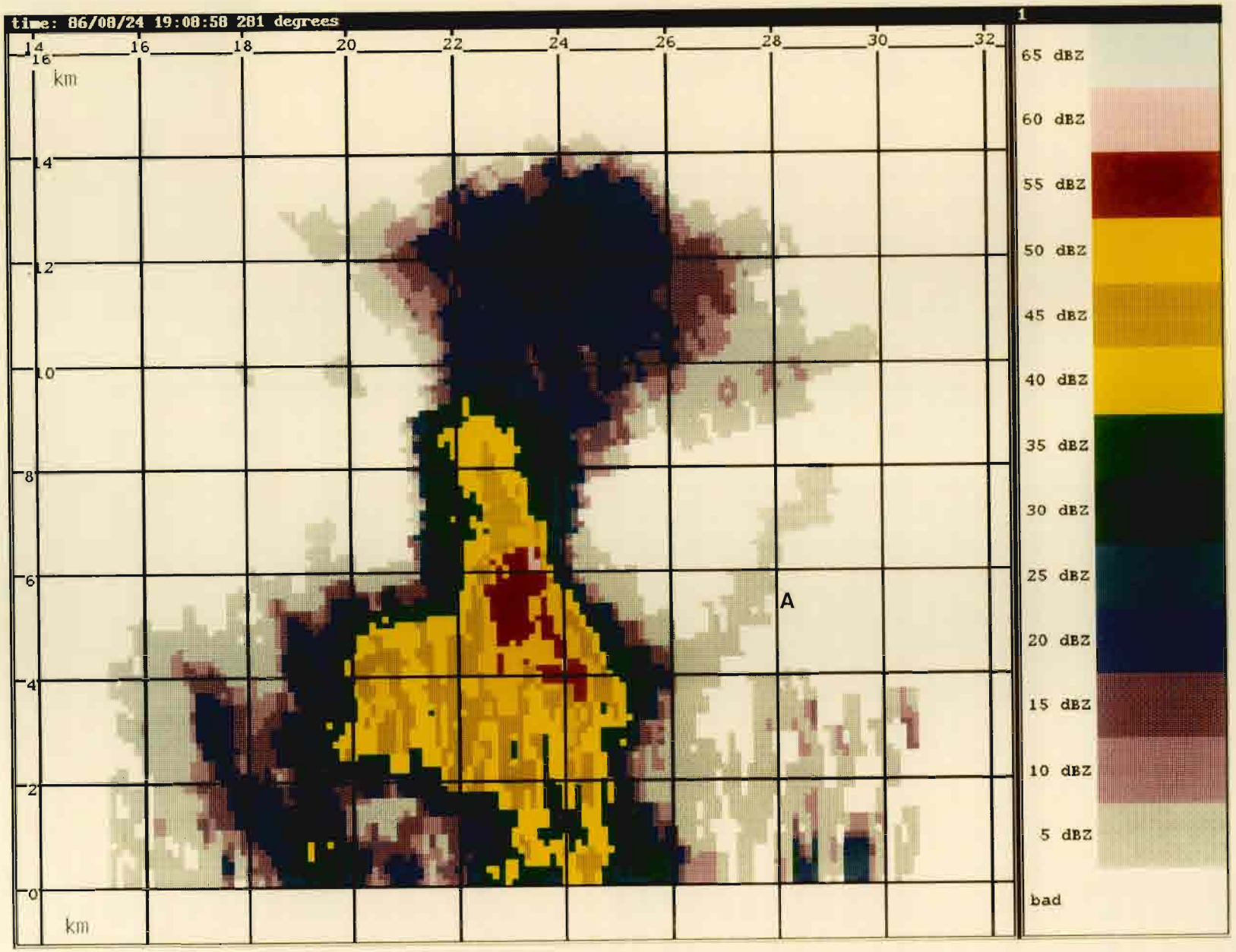

Figure III-10. RHI plot of Reflectivity Factor (190858 UTC)

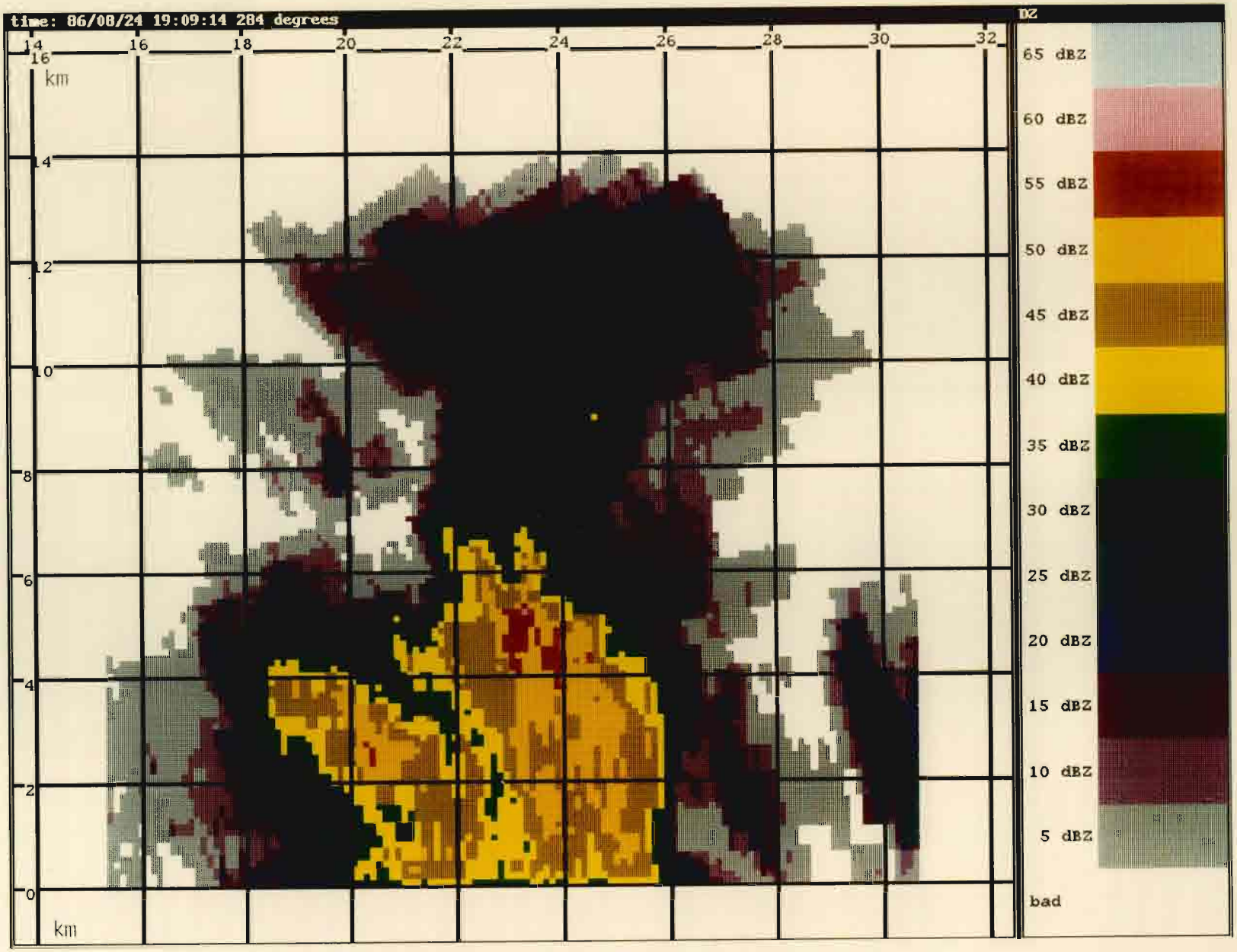

Figure III-11. RHI plot of Reflectivity Factor (190914 UTC)

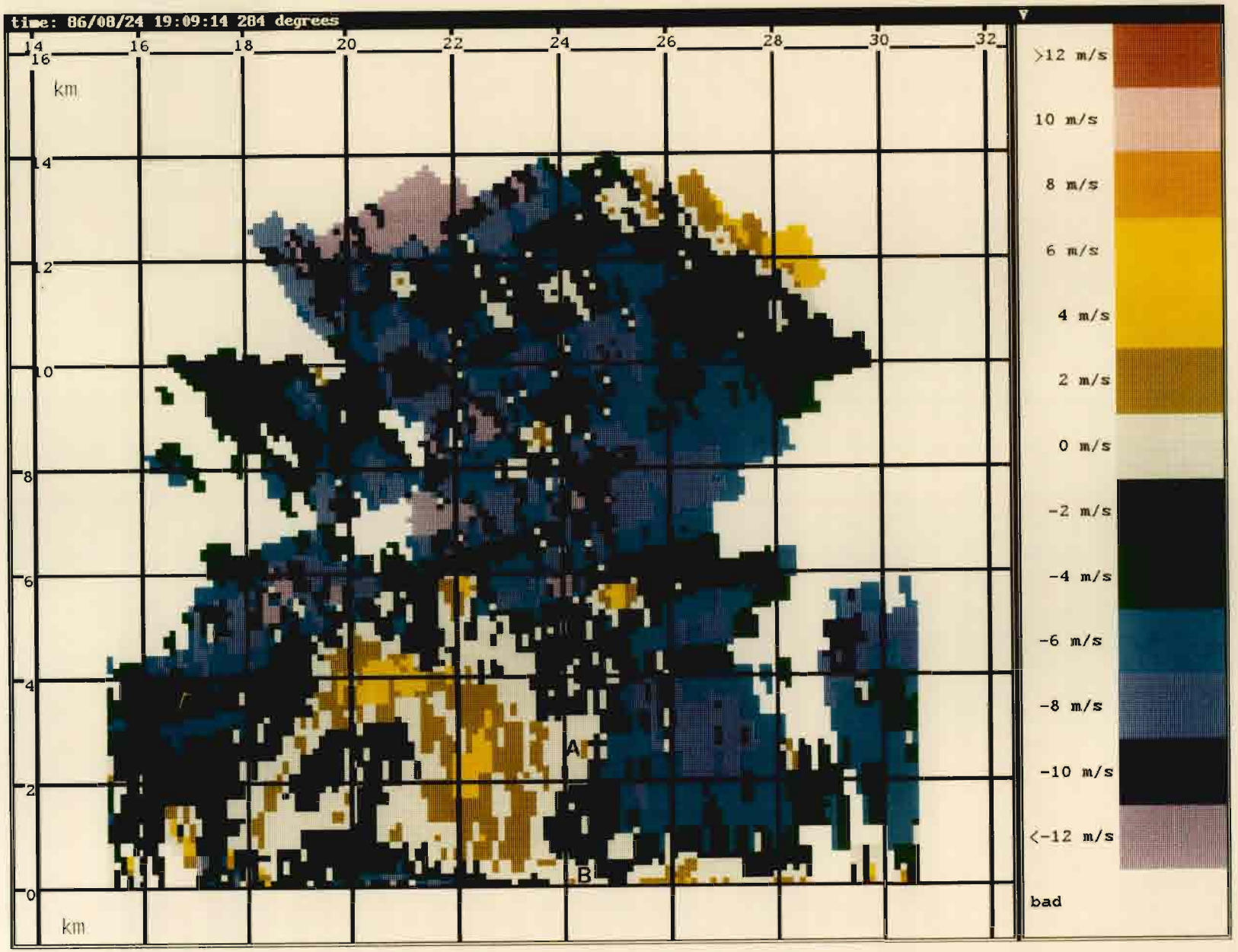

Figure III-12. RHI plot of Doppler Velocity (190914 UTC)

G. 191049 UT FEATURES

By 191049 the differential velocity in the outflow located at -23.1 km and 7 km (O) is 12 m/s (Figure III-13). The strongest winds are perpendicular to the major axis of the cell. This is consistent with results from Oklahoma (Eilts, 1987). The surface divergence is 17.5 x 10-3 s-1 which could be operationally significant to aircraft (Elmore et al., 1986). In Figure III-14, anticyclonic rotation exists at a height of 2 km above the microburst. The rotation is centered (R) along the western edge of the echo (-22.6 km, 5.1 km) with a maximum azimuthal shear of 7.5 x 10-3 s-1.

H. 191443 UT FEATURES

Figure III-15 is a vertical cut through the storm containing pertinent information at 3 levels. The cell has low-level divergence (A), mid-level convergence (B), and upper-level divergence (C). The divergent tops (27 m/s) and convergence (16 m/s) have intensified since 1910 UT. The flare (D) is still apparent at a height of 3.5 km. By 191454, the echo tops have fallen to 13.2 km (Figure III-16). Over a 5-min period, the 40 dBz contour has extended to 10.2 km AGL.

I. 191525 UT FEATURES

Figure III-17 is a dual-Doppler surface wind analysis at 191525. A divergent signature is centered on the northwestern edge of the echo. Most of the flow is to the east, south, and southwest. Due to cell movement, the divergent center is displaced from the storm's center. Figure III-18 is a streamline plot which indicates an outflow (A) centered at -21.3 km and 6.2 km. The surface divergence has decreased to 10 x 10-3 s-1. Rotation still persists (A) above the outflow (Figure III-19).

J. 191855 UT FEATURES

In Figure III-20 cell strengthening is apparent from the divergent tops (B) at 13.7 km AGL. The flare (A) is detected outside the core at a height of 2 to 5 km. In fact it has descended 1.5 km over a 10-minute period. A microburst with a peak differential velocity of 18 m/s is centered at 22 km and 278 deg. By 191901, the core has decreased in area by 50% over the last 4 minutes (Figure III-21).

K. 192054 UT FEATURES

A single-Doppler velocity plot at 192054 (Figure III-22) indicates anticyclonic rotation (A) located at 1.7 to 2.5 km AGL. By 192128 (Figure III-23), the microbursts size (3.5 km) and intensity (24 m/s) represents the greatest horizontal wind speed change with distance. An aircraft penetrating the echo from west to east would experience a 50 knot headwind/tailwind differential.

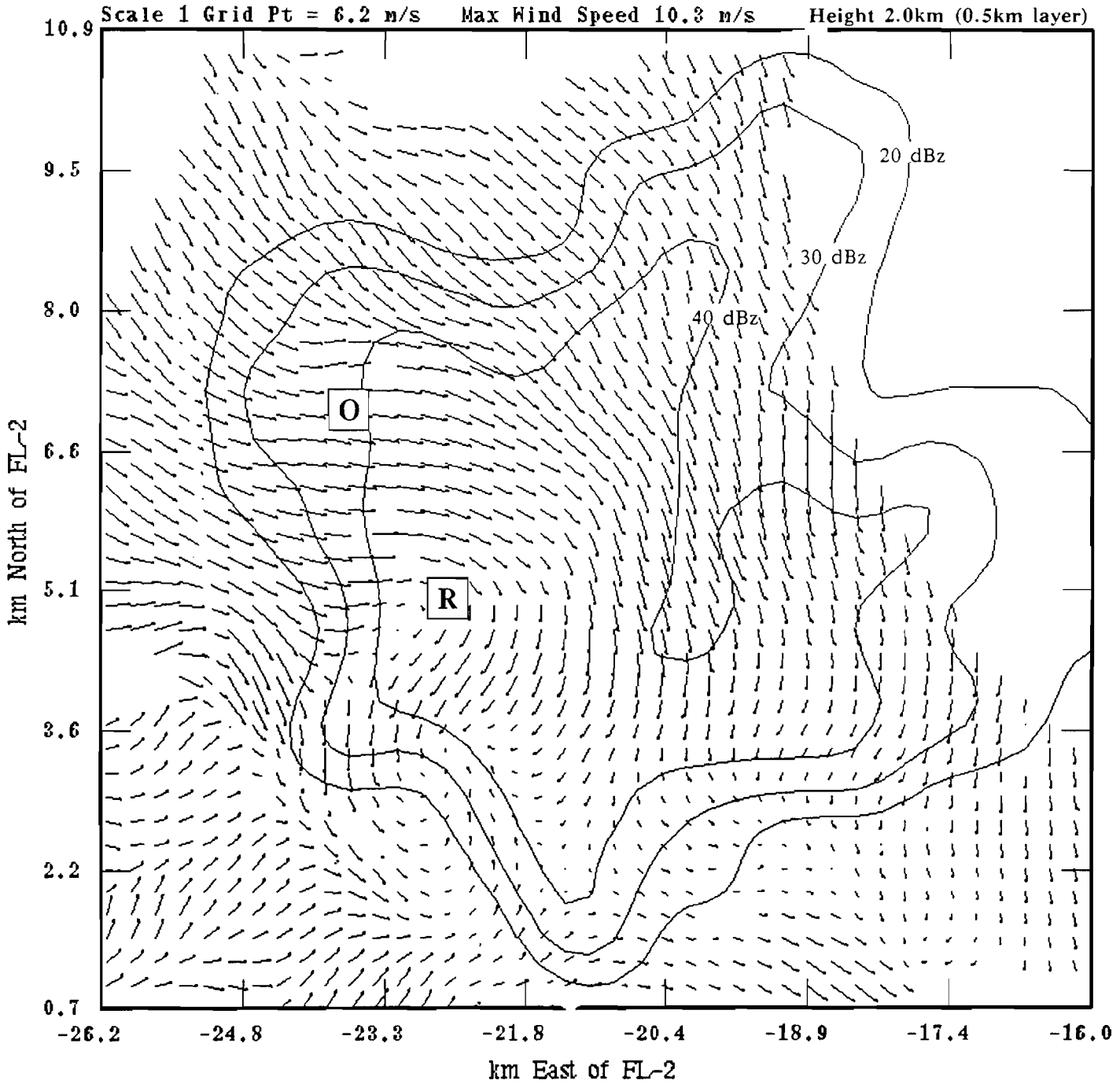

Figure III-14. Dual-Doppler Wind and dBz Plot (191059 UTC).

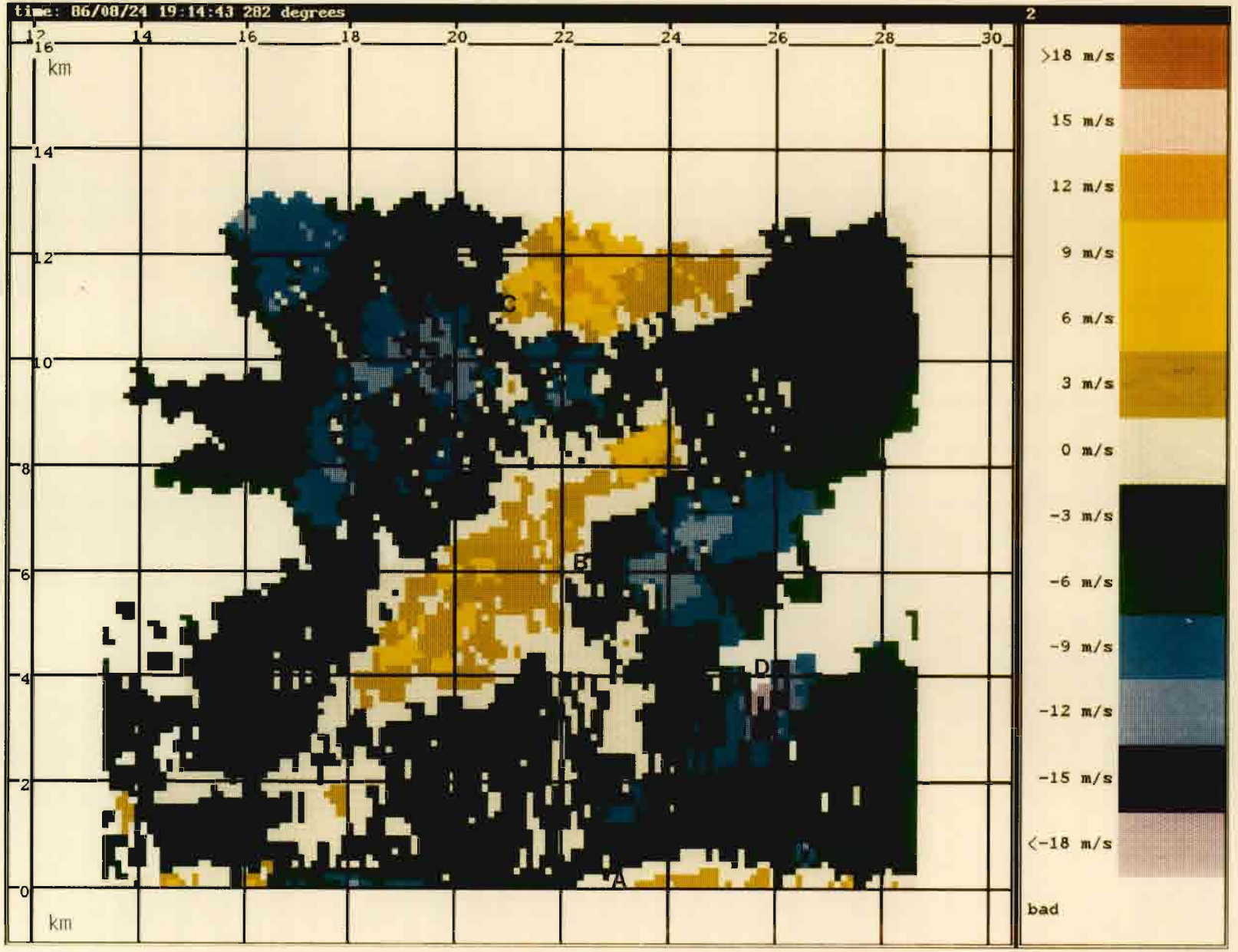

Figure III-15. RHI plot of Doppler Velocity (191443 UTC)

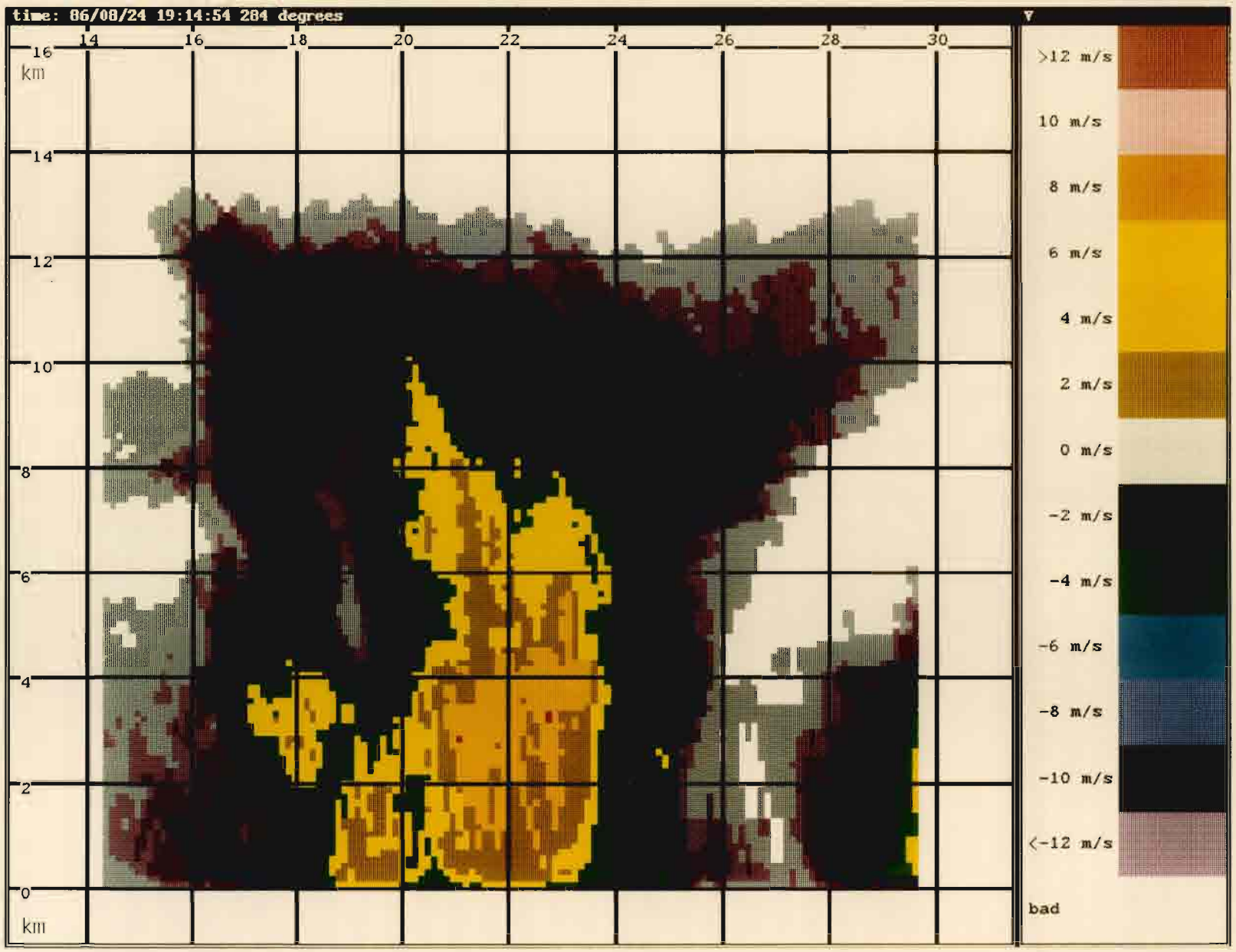

Figure III-16. RHI plot of Reflectivity Factor (191454 UTC)

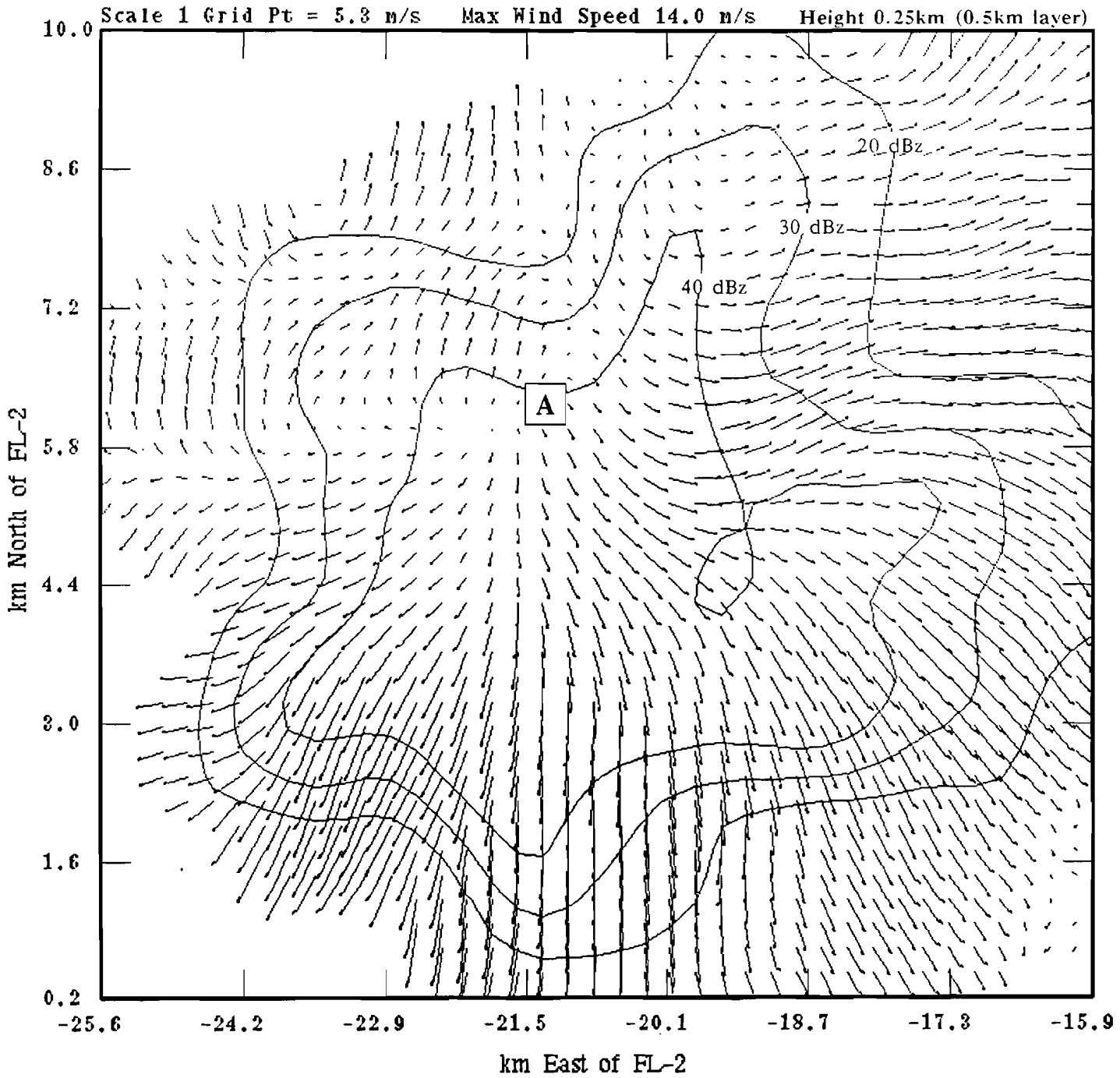

Figure III-17. Dual-Doppler Wind and dBz Plot (191525 UTC).

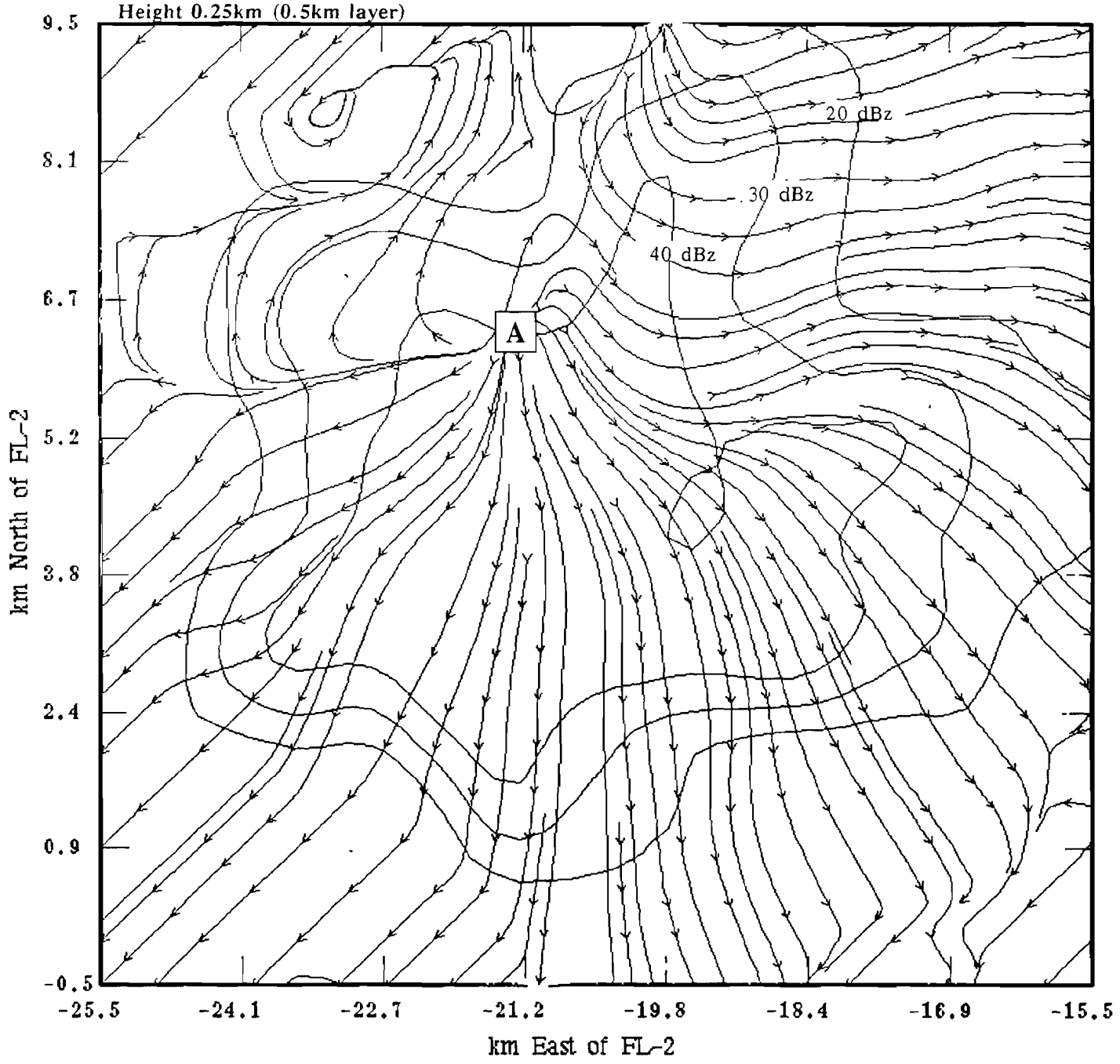

Figure III-18. Dual-Doppler Streamline Plot (191525 UTC).

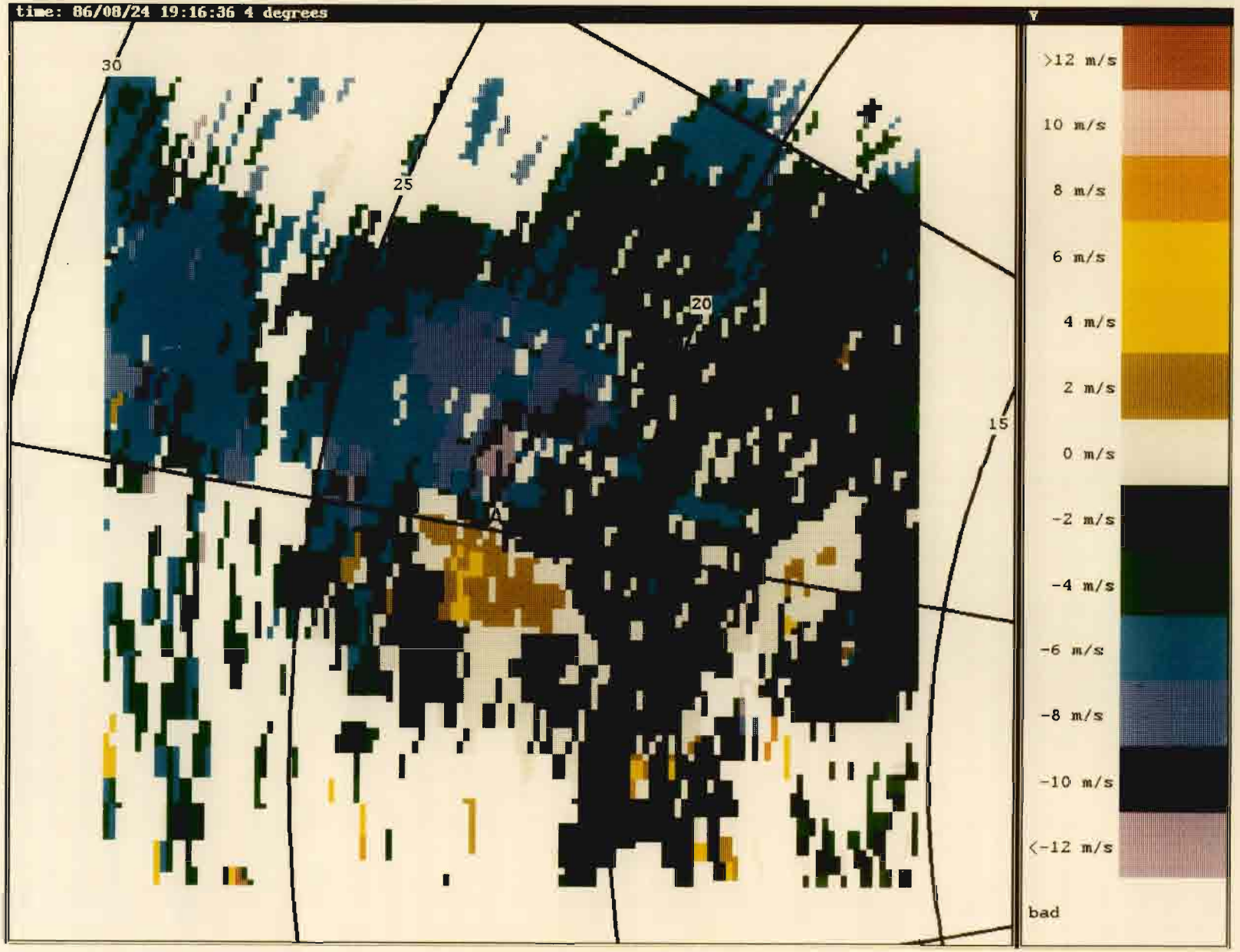

Figure III-19. PPI Plot of Doppler Velocity (191636 UTC)

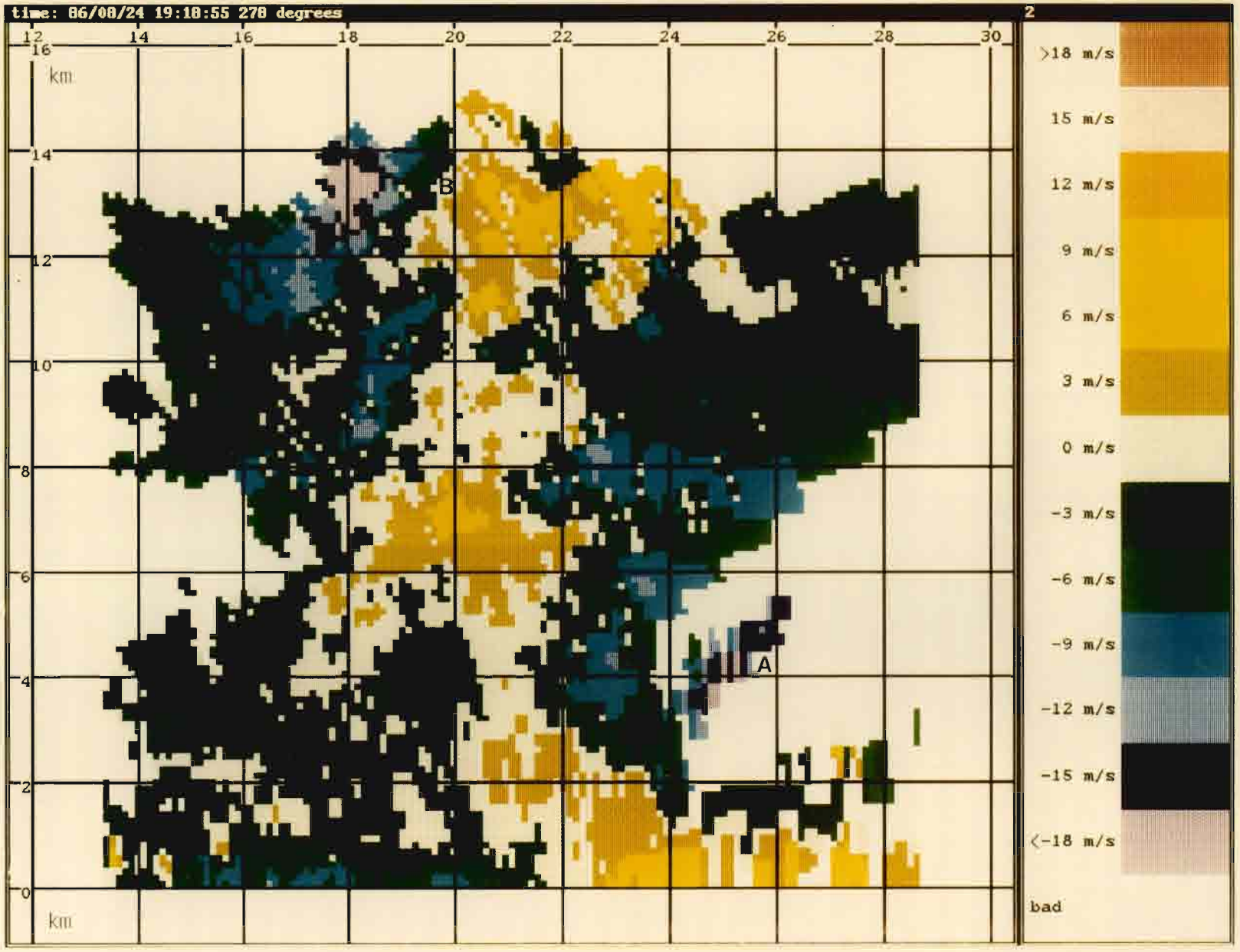

Figure III-20. RHI plot of Doppler Velocity (191855 UTC)

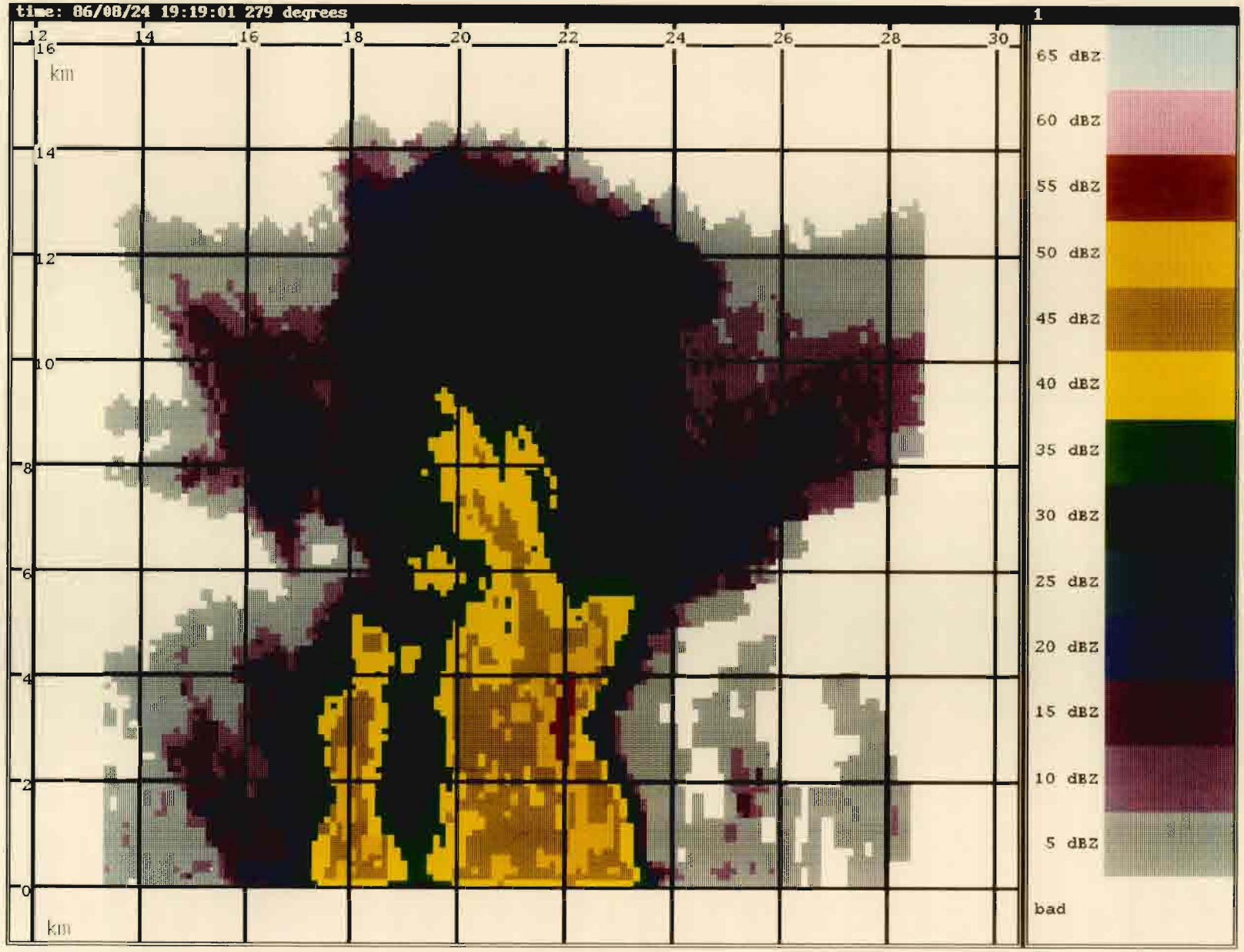

Figure III-21. RHI plot of Reflectivity Factor (191901 UTC)

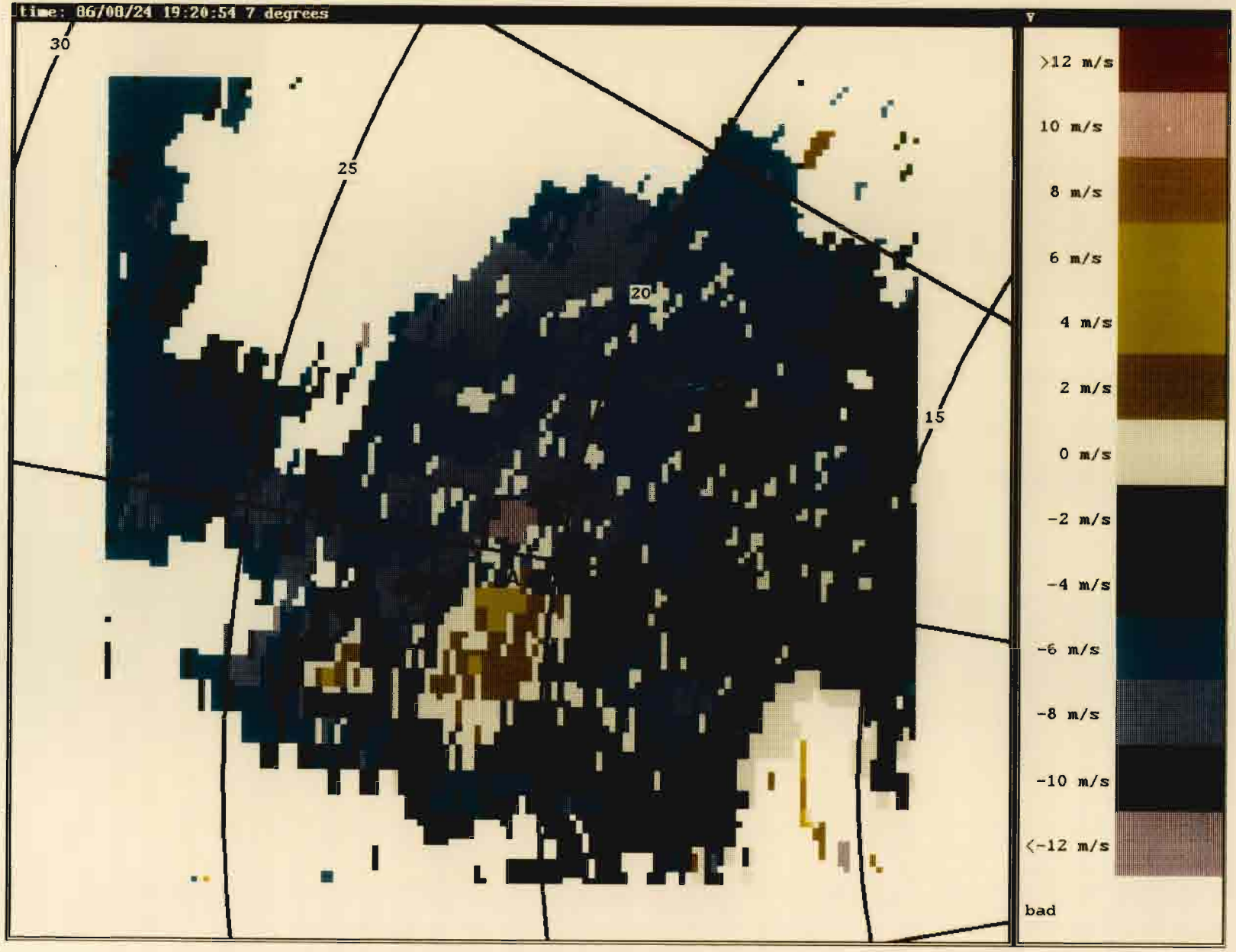

Figure III-22. PPI plot of Doppler Velocity (192054 UTC)

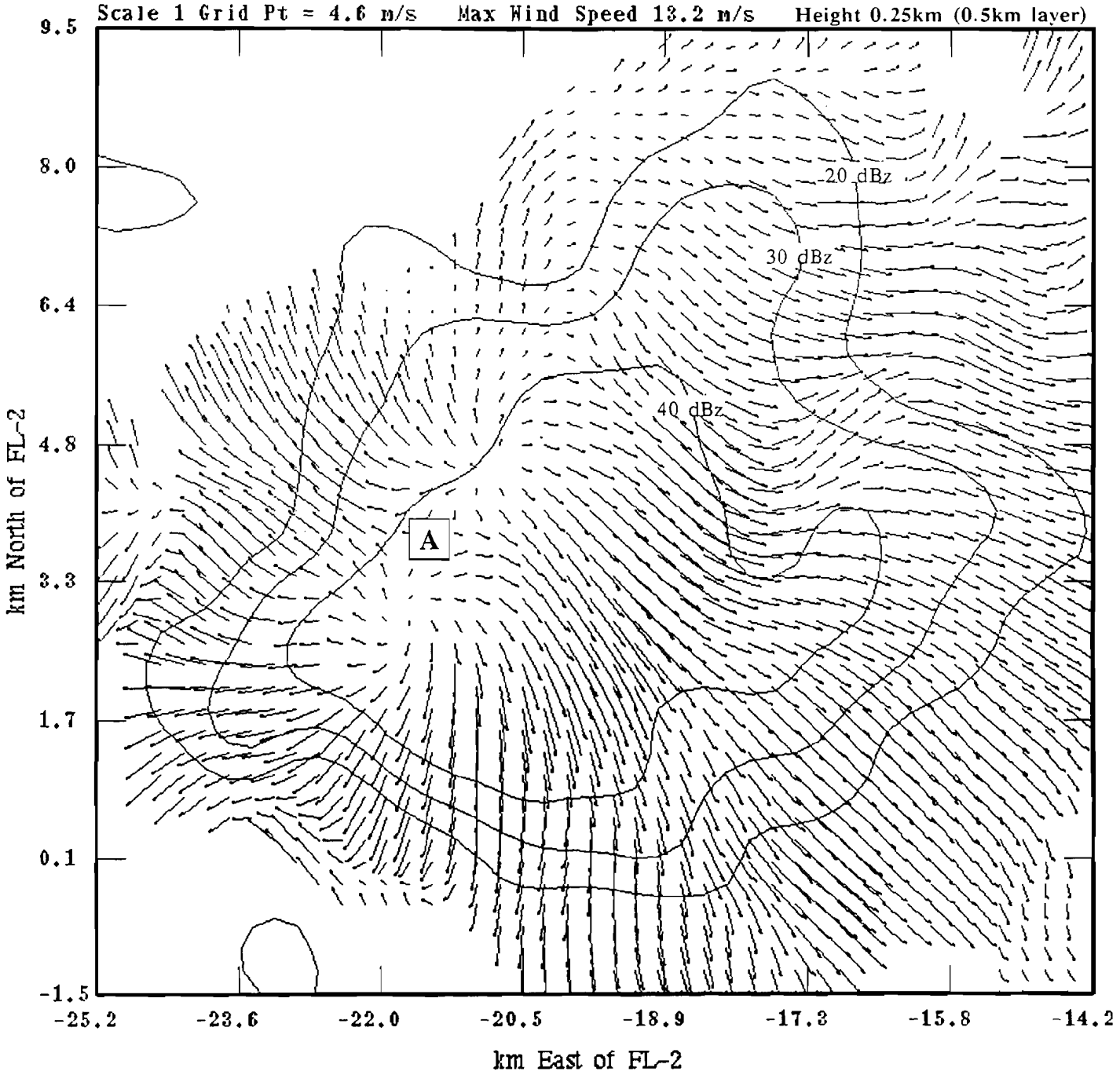

Figure III-23. Dual-Doppler Wind and dBz Plot (192128 UTC).

L. 192317 UT FEATURES

By 192317 (Figure III-24) the top of the core has dropped below the freezing layer and its areal extent has decreased significantly since 1914 UT. Echo tops are maintained at 14.6 km. Cell widening at upper-levels is a possible indication the storm is decaying. This event is similar to the high reflectivity model of Roberts and Wilson (1986) since it eventually progressed into a large-scale outflow.

M. 192349 UT FEATURES

The microburst is centered (A) on the western edge of the cell (Figure III-25). The maximum radial velocity difference is in an east to west direction. Figure III-26 is a PPI velocity tilt at 12 degrees elevation from the UND radar which indicates rotation (A) is still evident at an altitude of 2.3 km AGL. A velocity flare (B) persists at low-levels outside the cell.

N. 192735 UT FEATURES

By 192735, cell growth is no longer apparent (Figure III-27). There is only a small region of > 50 dBz echo and the storm tops have decreased to 13.1 km. The widening at the top of the cell suggests that the storm is transitioning into the dissipating stage.

O. 192806 UT FEATURES

A dual-Doppler surface wind analysis at 192806 (Figure III-28) displays a macroburst outflow with a surface divergence of 10 x 10-3 s-1 located (A) at -21.4 km and 1.2 km.

P. 193045 UT FEATURES

The final dual-Doppler plot (Figure III-29) indicates a flow pattern primarily in the direction of the prevailing winds eg., northwest to southeast.

IV. TIME-HEIGHT PROFILE

Further information on the vertical structure of the microburst producing cell can be obtained from a time-height (*) contour plot of the radar reflectivity factor (Figure IV-1). It was constructed by plotting the maximum reflectivity in dBz versus height for each radar volume scan between 1830 and 1930 UT. The closely-spaced contours at 1838 UT are due to extrapolation at the edge of the data region.

Reflectivities of 50 dBz first reach the surface 9 minutes prior to an outflow of 10 m/s. By 1905 UT, the core has reached a maximum depth of 7 km. After this time, the height of maximum reflectivity and core depth gradually decrease. There is a dip evident at the top of the reflectivity core (C) prior to the initial microburst outflow.

(*) This conception of a time-height profile is different from that proposed by Roberts and Wilson (1986). In their study of JAWS microbursts, areas above a fixed radar reflectivity factor were plotted versus time and height. The reflectivity threshold was defined as 10 dBz less than the maximum reflectivity within the storm.

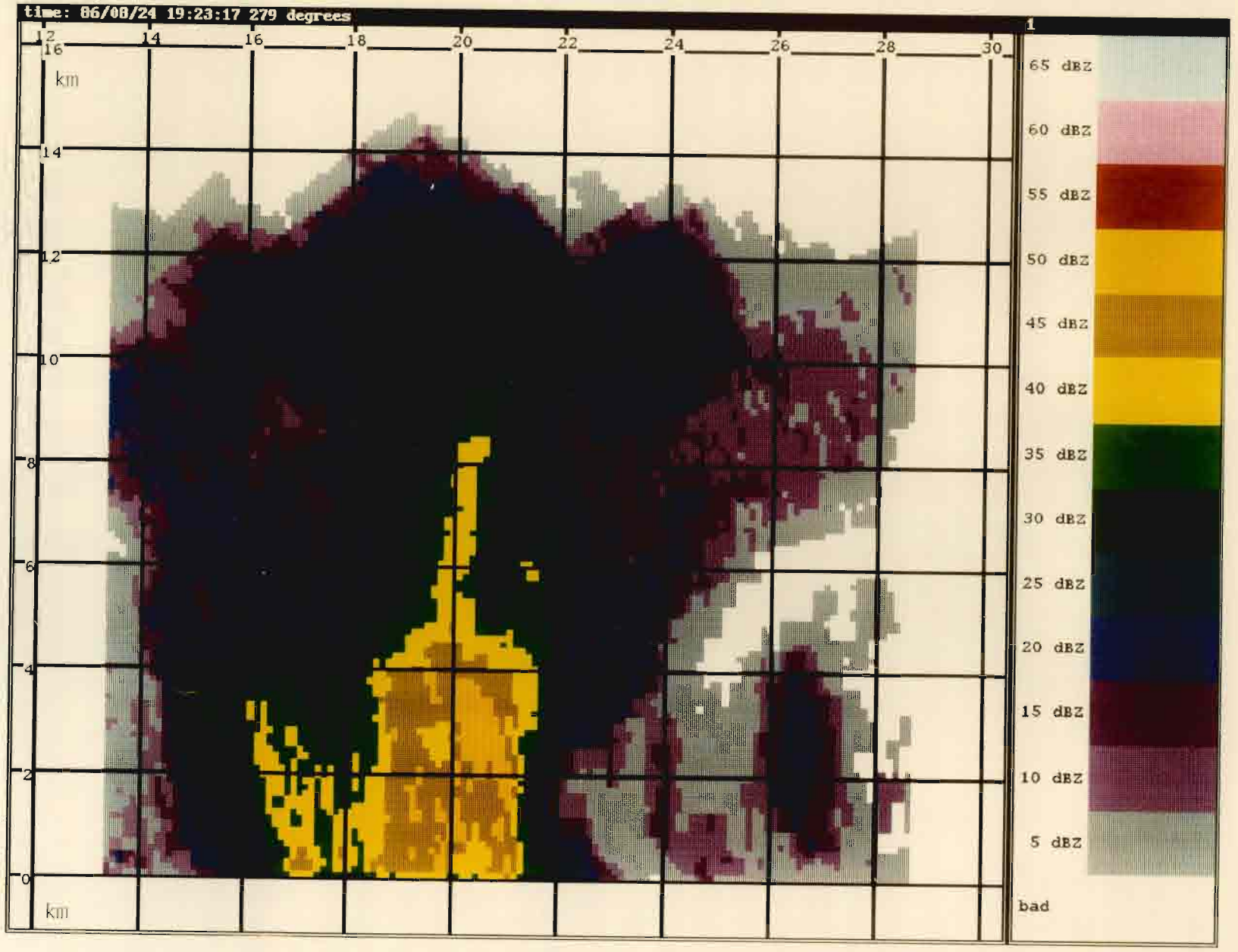

Figure III-24. RHI plot of Reflectivity Factor (192317 UTC)

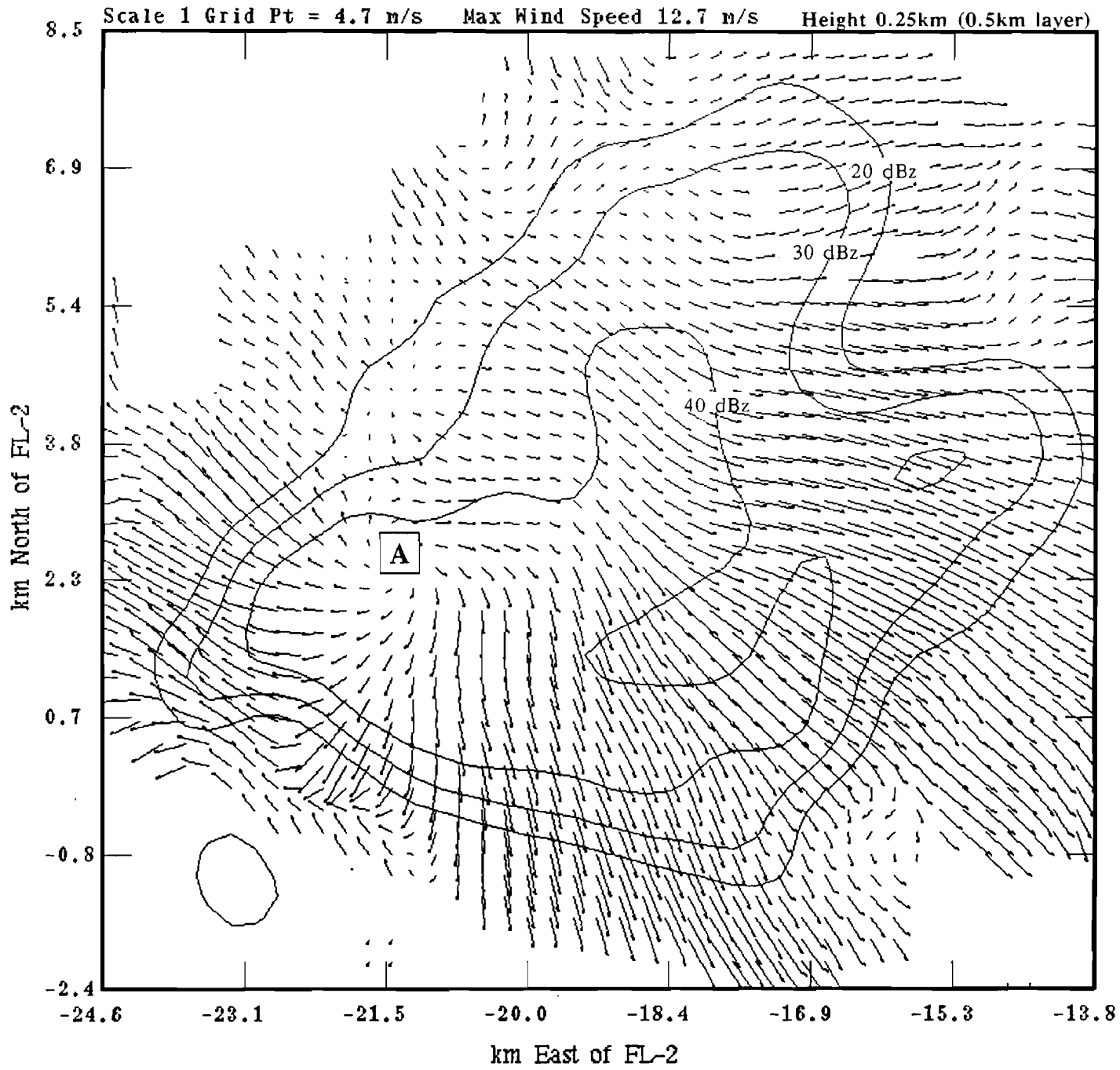

Figure III-25. Dual-Doppler Wind and dBz Plot (192349 UTC).

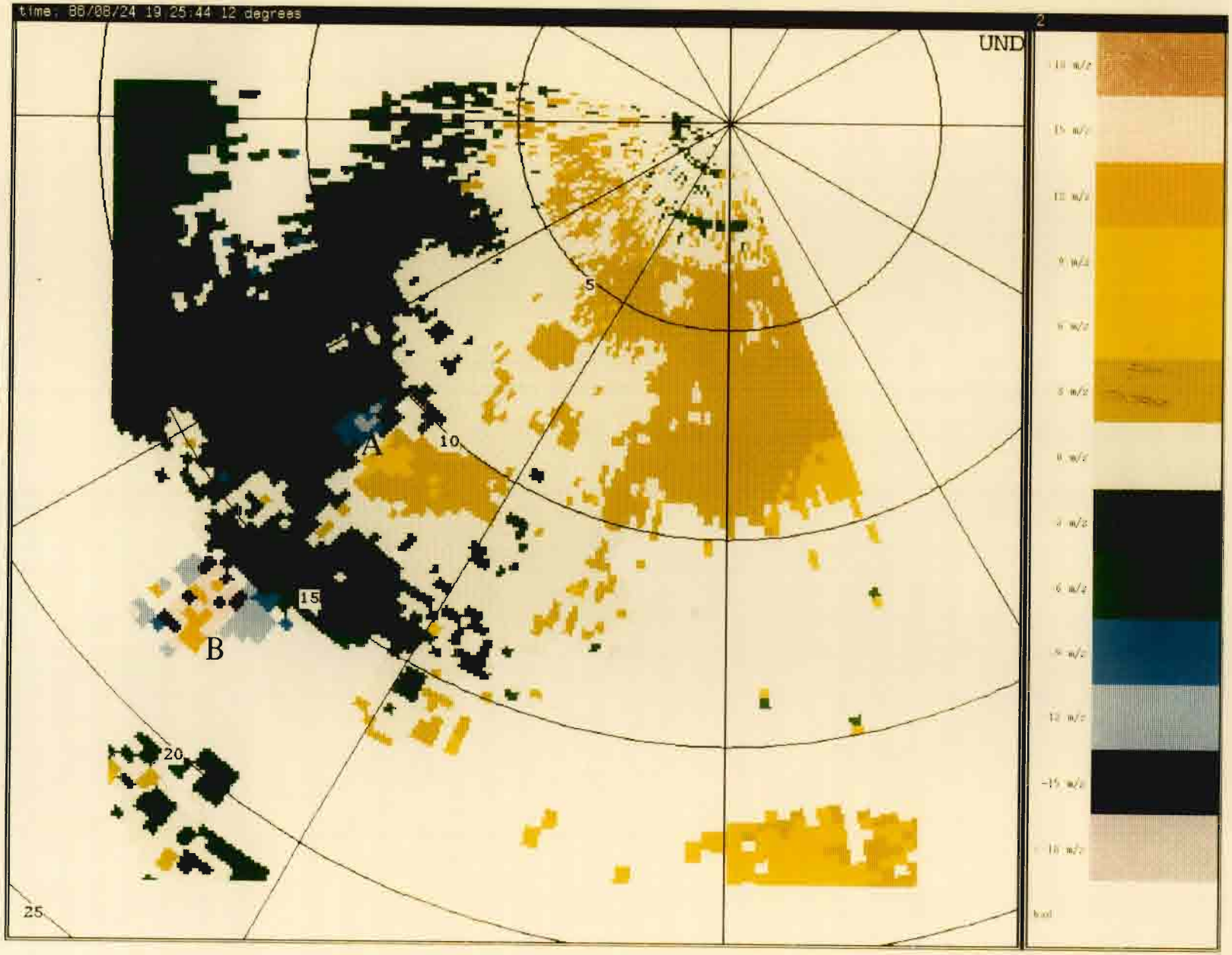

Figure III-26. PPI plot of Doppler Velocity (192544 UTC)

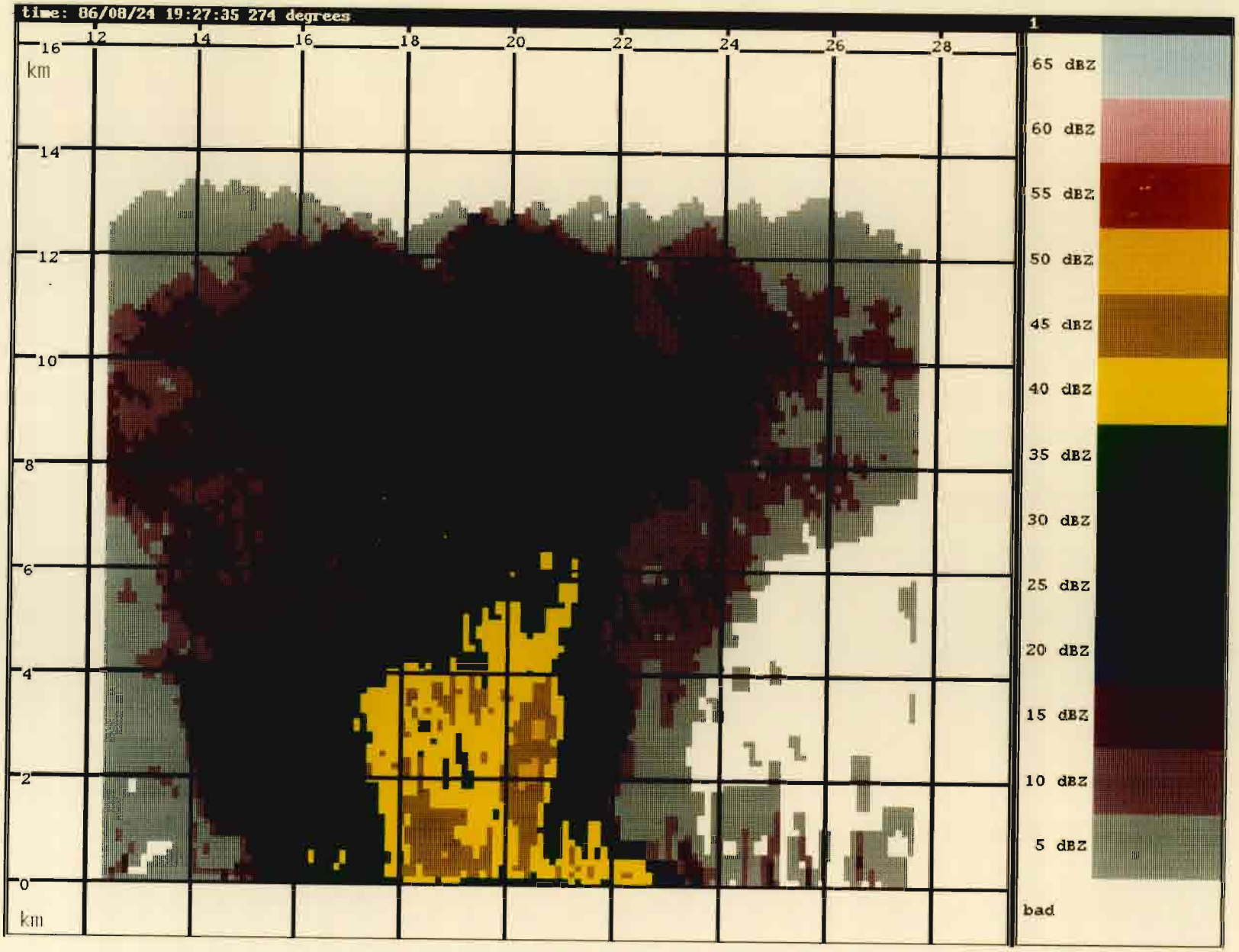

Figure III-27. RHI plot of Reflectivity Factor (192735 UTC)

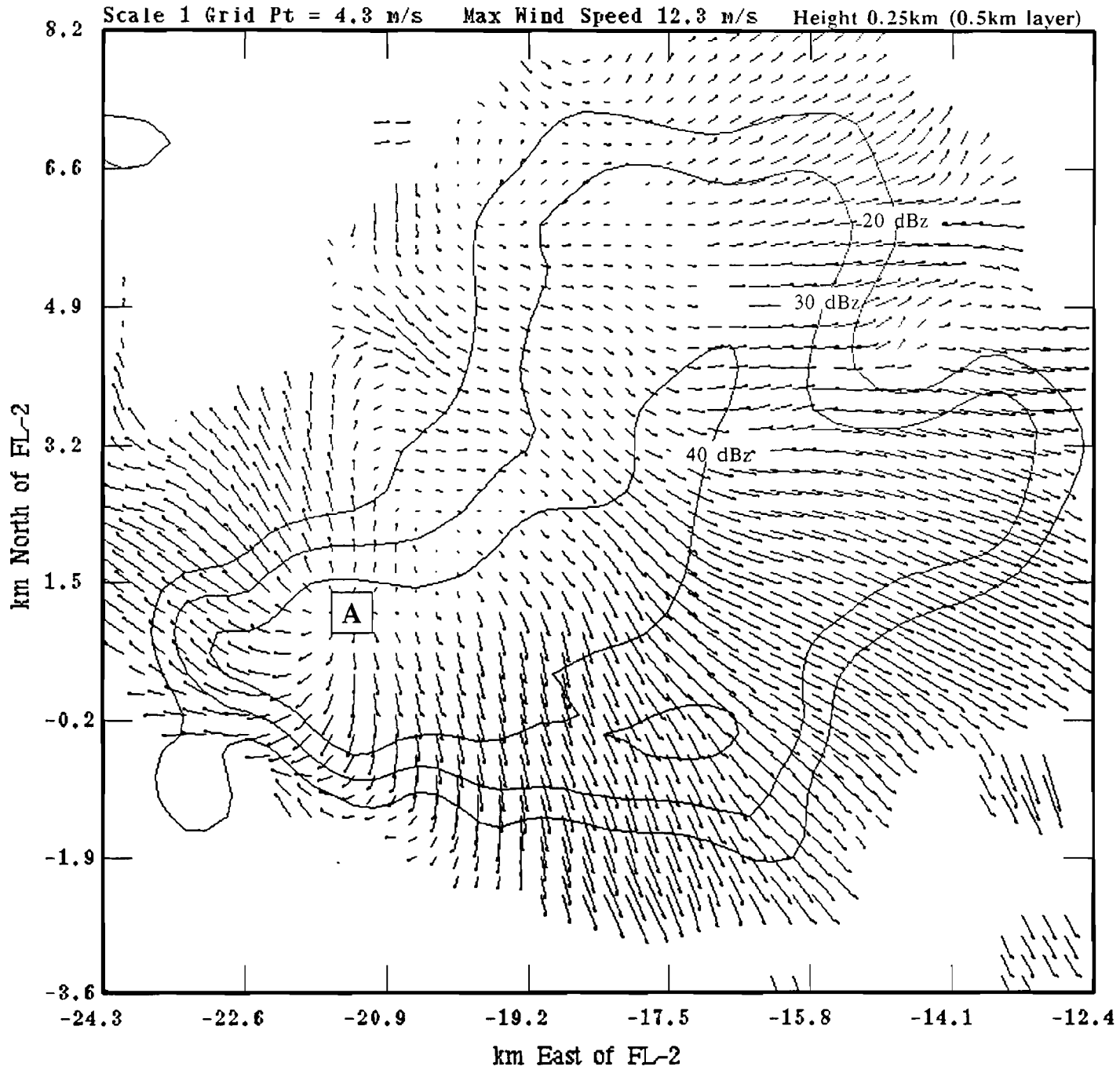

Figure III-28. Dual-Doppler Wind and dBz Plot (192806 UTC).

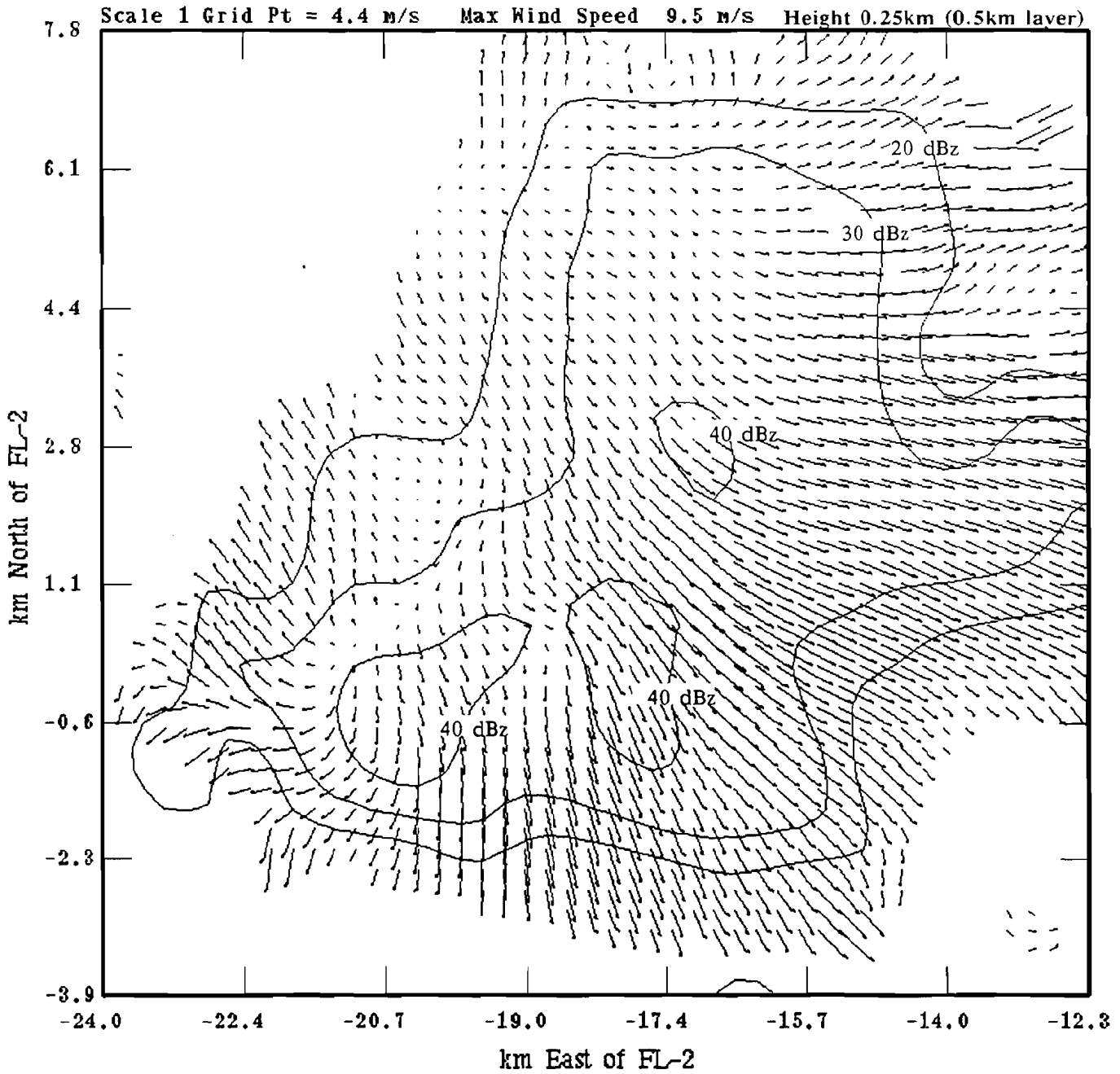

Figure III-29. Dual-Doppler Wind and dBz Plot (193045 UTC).

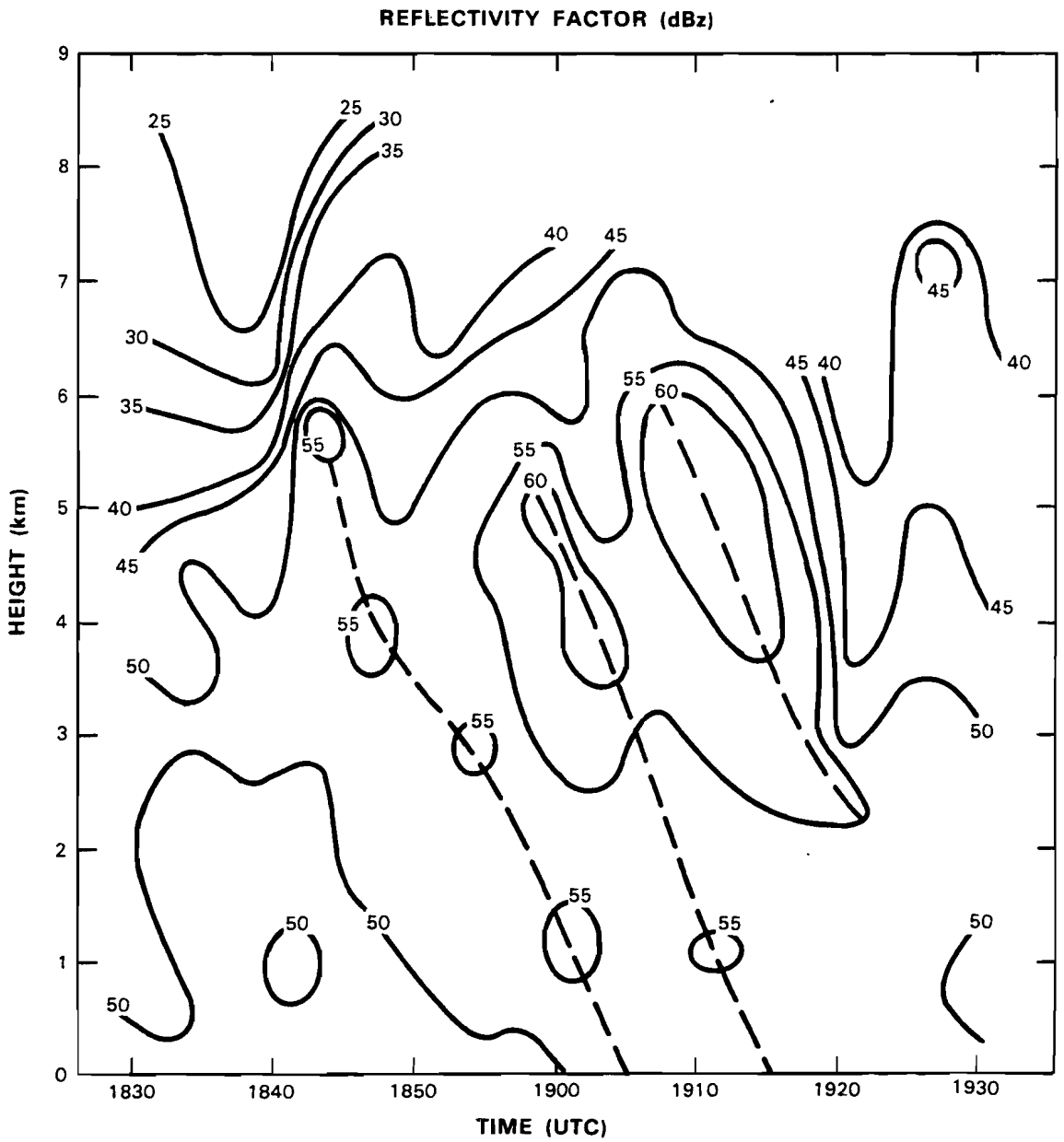

Figure IV-1. Time-Height Contour of Reflectivity Factor (dBz).

The initial reflectivity maxima developed at a height of 5.7 km (1842 UT) and descends to the surface by the time of initial surface divergence (A). A second region of strong reflectivities (60 dBz) formed between 3.5 and 5.0 km AGL 5 minutes before the initial divergence and descends to the surface 4 minutes prior to the microbursts peak intensity (B). In this case the outflow intensifies after the second reflectivity maxima reaches the surface. A third reflectivity maxima at 3.5 to 6 km AGL (1912 UT) appears to remain primarily aloft throughout the microburst life cycle. The descent rate (1.6 km/min) of the maximum reflectivity is similar to the high reflectivity model in Roberts and Wilson (1986). For over 1 hour, the storm maintains reflectivities of > 50 dBz.

Figure IV-2 is a plot of the maximum velocity for each volume scan that a feature was detected. Mid-level rotation first occurs 23 minutes before the surface outflow and persists throughout the lifetime of the event. Upper-level divergence was initially detected 18 minutes prior to a 10 m/s outflow. Between 1900 and 1922 UT, convergence is detected at mid-levels in the storm. Each of the velocity features peaked at or before the maximum surface divergence. Studies are in progress to determine if the outflow strength can be estimated based on the intensity of convergence, rotation, or divergent tops. It would also appear that the reflectivity maxima may be useful for core tracking. Table IV-1 summarizes the velocity features observed in this microburst. The most dominant feature aloft in terms of total detections was mid-level rotation.

V. DEPTH OF OUTFLOW

The variability in outflow depths is pertinent to the TDWR scan strategy and siting. In particular, the radar could underestimate or miss the microburst if the beam is above the height of maximum velocity change. DiStefano (1987) reported a shallow depth of outflow as a contributing factor for a missed microburst by the FL-2 radar on 23 July 1985 in Memphis, Tennessee.

Rinehart et al. (1987) reported an average microburst depth of approximately 500 meters for 14 Memphis outflows. Typical outflow depths for JAWS microbursts varied between 500 and 800 meters (Roberts and Wilson, 1984 and Hjelmfelt, 1987). In this study, the depth of outflow is defined as the height at which 1/2 the maximum surface velocity is observed. For more information on this parameter refer to Rinehart et al. (1987).

At 190930, the depth of outflow was calculated as 440 meters. The maximum velocity extends from the surface to 200 meters. By 191845 the depth had increased to 540 meters. At this time the radial divergence exceeds 10 m/s from the surface to 380 meters. Five minutes later, the depth of outflow was 440 meters. The outflow reached a maximum depth at the same time as the peak microburst velocity.

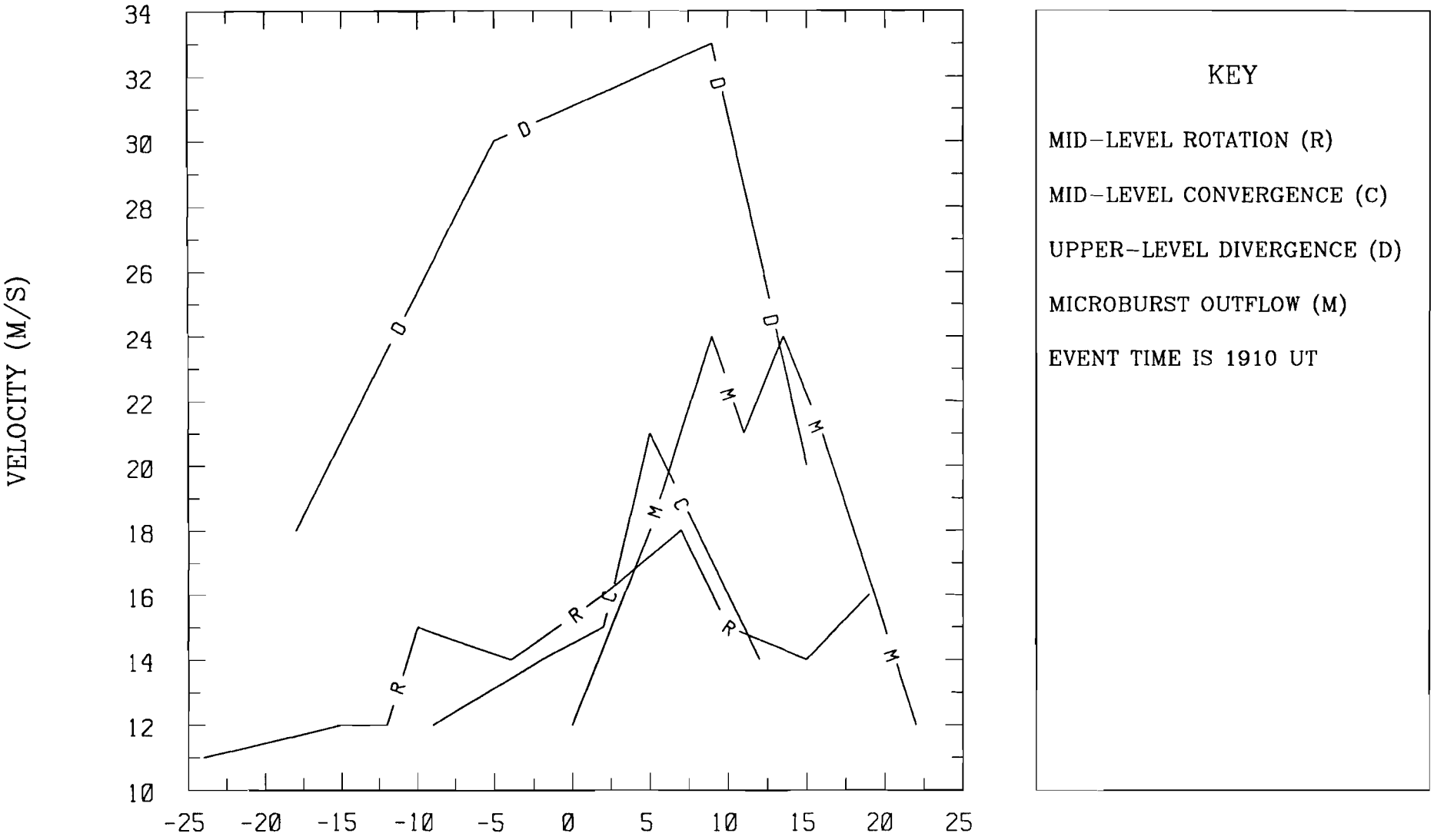

Figure IV-2. Time-Height Profile/Velocity Features

Figure IV-2. Time-Height Profile/Velocity Features.

Table IV-1. Summary Of 24 August 1986 Features Aloft

Time UT	Scan Mode	Feature Aloft	Location ran/az	Deltav m/s	Height km
184634	PPI	Rotation	29/296	11	2.8
185228	PPI	Divergence	29/295	18	7.9
185455	PPI	Rotation	28/292	12	3.6
185510	PPI	Rotation	28/294	10	4.1
185836	PPI	Rotation	26/291	12	2.1
185847	PPI	Rotation	26/291	12	3.0
185859	PPI	Rotation	26/291	12	3.9
190058	RHI	Convergence	26/296	12	5.0
190017	PPI	Rotation	26/293	15	5.1
190303	PPI	Rotation	24/289	12	2.7
190314	PPI	Rotation	24/289	12	3.2
190455	RHI	Divergence	25/291	30	11.0
190609	PPI	Rotation	24/287	12	0.7
190620	PPI	Rotation	24/287	12	1.3
190632	PPI	Rotation	24/290	14	1.7
190643	PPI	Rotation	24/286	14	2.1
190717	PPI	Rotation	24/290	10	3.0
190729	PPI	Rotation	24/291	10	3.4
190740	PPI	Rotation	23/290	10	2.3
190752	PPI	Rotation	23/283	12	3.5
190803	PPI	Rotation	23/287	10	4.0
190813	PPI	Rotation	22/282	12	4.7
190823	PPI	Convergence	24/284	14	4.9
191151	PPI	Rotation	23/283	12	1.4
191204	PPI	Rotation	23/282	14	1.8
191216	PPI	Rotation	23/283	16	2.3
191216	PPI	Convergence	23/282	15	2.3
191229	PPI	Rotation	23/283	14	2.8
191241	PPI	Rotation	23/283	14	3.2
191443	RHI	Convergence	21/283	21	5.1
191624	PPI	Rotation	22/281	12	1.1
191636	PPI	Rotation	22/282	14	1.7
191647	PPI	Rotation	22/281	18	2.2
191659	PPI	Rotation	22/281	16	2.6
191710	PPI	Rotation	22/281	12	3.2
191917	RHI	Divergence	21/282	33	14.0
191932	PPI	Rotation	21/282	14	2.6
192009	PPI	Rotation	21/284	15	3.5
192031	PPI	Divergence	23/283	20	11.3
192054	PPI	Rotation	21/279	12	2.6
192118	PPI	Divergence	22/282	18	9.9
192140	PPI	Rotation	21/278	14	1.8
192200	PPI	Convergence	21/278	14	2.5
192226	PPI	Rotation	22/277	15	0.9
192238	PPI	Rotation	20/274	16	4.1
192448	PPI	Divergence	23/274	20	10.9
192512	PPI	Rotation	20/277	14	2.4
192558	PPI	Rotation	20/276	14	1.6
192643	PPI	Rotation	20/274	10	0.8
192844	PPI	Rotation	19/274	16	3.1
192928	PPI	Rotation	19/273	14	2.3

VI. MICROBURST ASYMMETRY

One limitation of a single Doppler radar is to estimate the headwind-tailwind shear along a flight path when the beam is not parallel to the runway. If the radar is viewing the minimum radial velocity axis, an outflow might go undetected or underestimated. Previous studies [(Eilts (1987), Wilson et al. (1984), and Hjelmfelt (1987)] identified and calculated microburst asymmetries in Oklahoma and Denver. They reported worst case shear ratios of 6 times when comparing the maximum and minimum axis over a fixed distance, while the typical difference was 2 to 3. Thus it is essential to analyze this aspect of southeastern United States microbursts to determine if similar results are encountered.

A simple radial approach to estimate asymmetry is to compare velocity differentials from two radars. Figure VI-1 is a radial velocity plot of the 24 August microburst versus time for FL-2 and UND. The curves are essentially identical, only displaced by 7 or 8 minutes. The radial velocity difference varies less than 5 m/s over most of the plot. The largest deviation is noted during the latter stages of the outflow. From the FL-2 perspective, the microburst peaks 14 minutes after initial detection.

Another method of estimating asymmetry is calculating the ellipticity of the reflectivity field major and minor axes. Eilts and Doviak (1987) speculated that the shape of the reflectivity contour might be a useful symmetry parameter. In general, the more elliptical the cell the more asymmetrical the outflow. In Figure VI-2, the curve for average ellipticity is similar to the FL-2/UND radial velocity ratio between 1905 and 1925 UT. Once again there is less agreement in the latter stage of the event. During a 20-minute span, the over or under-estimation of radial velocity based on the average ellipticity ratio would not exceed 20%.

The best approach for calculating asymmetry is to compute the differential velocity from the dual-Doppler wind field. A technique has been developed at Lincoln Laboratory to calculate asymmetry similar to that presented in Wilson et al. (1984) and Eilts and Doviak (1987). One option computes the velocity differential at specified azimuths through the center of a microburst from the U and V wind component. For these analyses, an azimuthal increment of 10 degrees was applied between 0 and 180 degrees. A fictitious radar was located at a distance of 15 km from the center of the outflow. At 191049 the ratio of maximum to minimum velocity was 2.97, with a maximum of 22.6 m/s and a minimum of 7.6 m/s. The ratio decreased to 1.94 between 191525 and 192349 UT. The symmetry of the outflow increased throughout the microbursts life cycle. In most cases, the minimum velocity differential through the dual-Doppler wind field was < 10 m/s. It is possible that the event would go undetected if the radar was viewing the axis of minimum velocity differential. The asymmetry ratios reported here are similar to those for typical microbursts in Denver and Oklahoma.

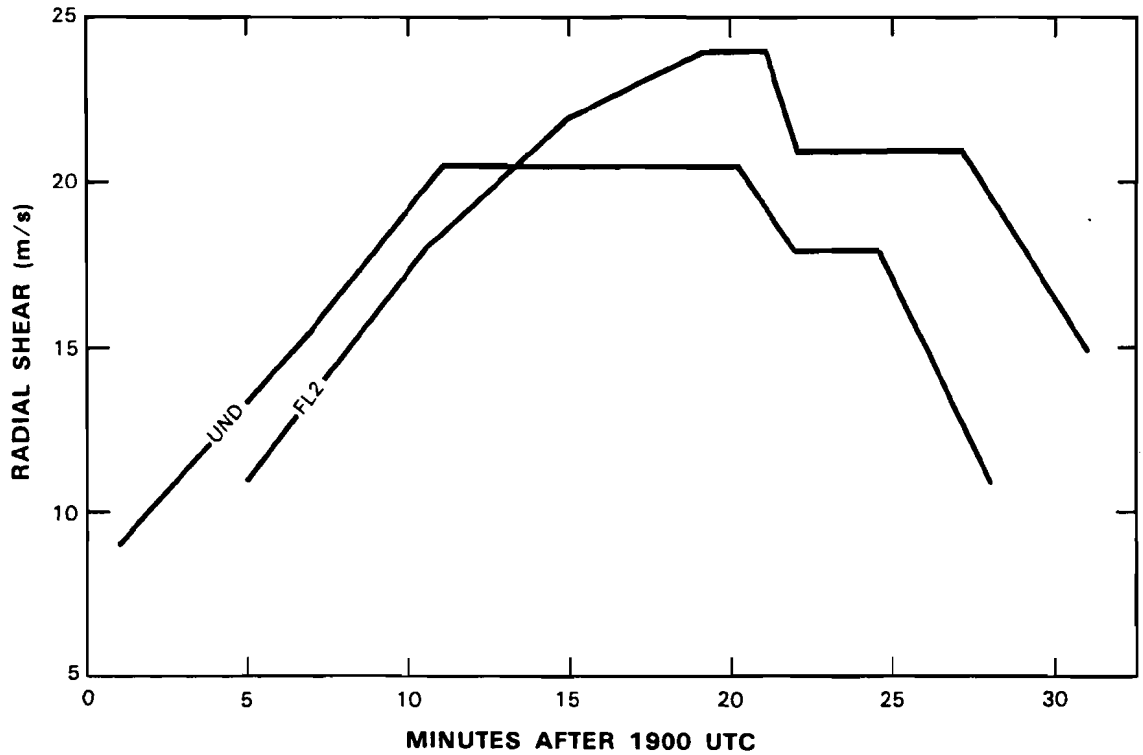

Figure VI-1. Radial Shear Plot vs. Time.

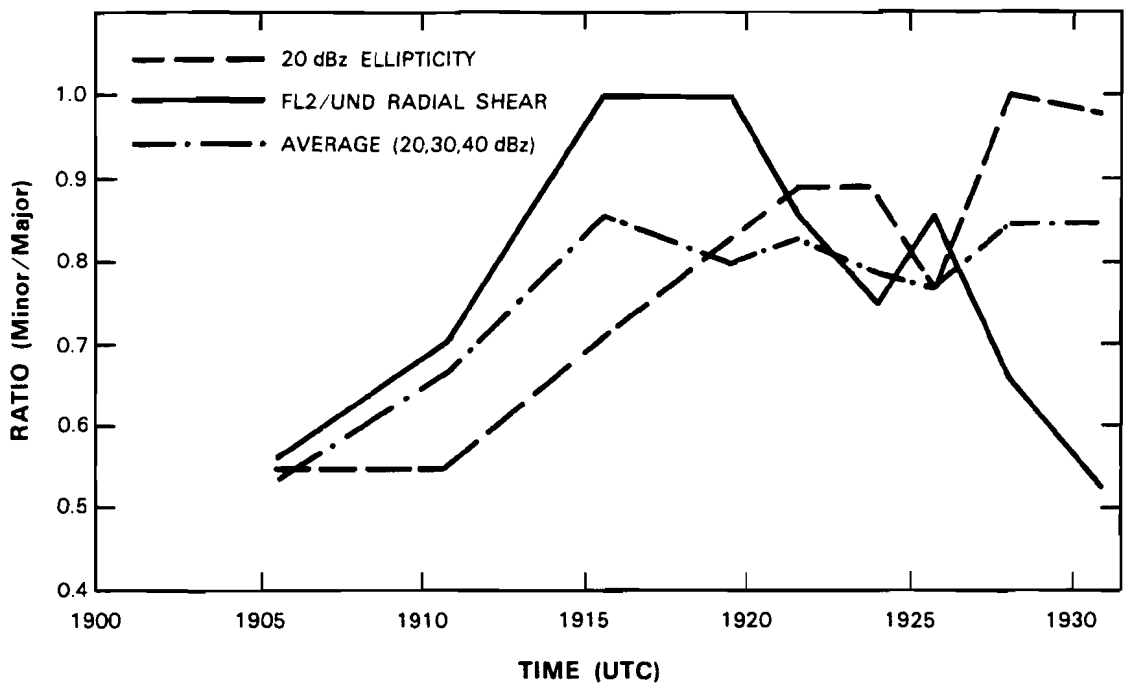

Figure VI-2. Radial Shear/Ellipticity Plot vs. Time.

VII. MICROBURST FORCING MECHANISMS

This section will consider possible microburst forcing mechanisms. Among those proposed are the collapse of overshooting tops, precipitation loading (ice and/or water), sub-cloud evaporation, in-cloud evaporation, cooling of air by melting precipitation, and vertical pressure gradients. Kessinger et al. (1986) alluded to the significance of evaporation in the downdraft process in dry sub-cloud regions. Roberts and Wilson (1984) discussed three primary classes of forcing mechanisms in the Denver area: 1) high-based shallow convective clouds were dominated by sub-cloud evaporation and melting, 2) well-defined descending precipitation cores are enhanced through the process of dry air entrainment at mid-levels, and 3) large hail-generating storms are influenced by precipitation drag, melting below cloud base, and the evaporation of water shed from hailstones. Studies in wet environments such as Oklahoma and Memphis identified these and other forcing mechanisms. Eilts (1987) maintained that initiation mechanisms in Oklahoma downburst included low altitude melting and evaporation of precipitation, precipitation loading, and evaporative cooling at mid-levels due to dry air entrainment. A study of a Memphis microburst on 10 August 1985 by Burrows and Osborne (1986) concluded that precipitation loading was a significant factor but may not have been sufficient to cause the downdraft without a contributing mechanism.

One possible forcing mechanism for the 24 August downburst was precipitation loading. This is supported by:

1) the high reflectivity (62 dBz) within the core three minutes before the outflow indicates the presence of large water droplets and/or ice at 3-4 km AGL,
2) an abundance of low-level moisture as reflected by the Nashville sounding would minimize the evaporation process below cloud base,
3) the potential for ice/water loading aloft is related to the flare which persists for 10-15 minutes, and
4) the enlargement of the core at 1900 UT played a significant role in the loading process.

On the other hand, reflectivity notching at mid-levels is possibly related to either the descent or evaporation of larger hydrometeors. Entrainment of drier air into the cloud at mid-levels could have served to enhance melting of the ice below the freezing layer and in-cloud evaporation. The relative importance of each mechanism could not be determined since detailed microphysical studies and/or a comparison of the temperature and humidity profile at the surface are required to accomplish this. There were no airplane measurements or surface mesonet data on this microburst.

VIII. MICROBURST ALGORITHM DETECTION CAPABILITY

This section will examine the detection capability of the microburst algorithm with and without features aloft. The current TDWR microburst detection algorithm only considers descending cores, lower divergence, divergent tops, rotation, and convergence as precursor mechanisms. This and other studies have alluded to the possible significance of features such as reflectivity notching, sinking tops, rapid vertical growth, and hail flare descent (Fujita, 1987). Several of these clues were evident in the 24 August 1986 microburst case. For one, the rapid vertical growth of the cell (12 m/s) occurs 5 minutes before the initial outflow. Secondly, the descent of the flare with time might be indicative of a descending core.

The timing of each feature detected in the radar data is discussed in relation to the initial outflow (1910 UT), the peak (1919 UT), and the reintensification (1923 UT). A mid-level feature (rotation) is first detected 24 minutes before the microbursts impact. Approximately 10 minutes prior to the initial divergence a core has descended below 2 km AGL (Figure IV-1). The combination of features aloft and weak surface divergence could have provided an early clue of an impending wind shear. At 1904 UT the core has descended to the surface and upper-level diverge has intensified. By this time, the preponderance of features aloft is a strong indication a microburst is imminent.

Next we will compare the performance of the features aloft (3-dimensional) and surface microburst detection algorithms to determine if the 3-dimensional version provides an earlier declaration of the event. The microburst producing cell is first detected by the advanced algorithm at 1825 UT. Ten minutes later a mid-level feature (rotation) is identified. The system distinguishes a reflectivity core aloft at 1853 UT which in combination with rotation at mid-levels is sufficient for the algorithm to declare a mid-level precursor. By 1901, a microburst is declared based on the identified precursor (rotation and reflectivity core) in combination with a weak surface outflow of 8 m/s. The core is recognized as descending at 1905 UT since it has fallen below 2 km AGL. Upper-level divergence is first detected at 1921 UT once the PPI scan strategy extended to the top of the echo. Throughout the microburst life cycle, the features aloft algorithm consistently detects both middle and upper-level precursors including rotation, divergence, and a reflectivity core. In comparison, the surface version of the microburst algorithm first identifies the event two surface scans later (1910 UT). For this case-study, the 3-dimensional algorithm provides an earlier declaration of the microburst.

IX. SUMMARY AND CONCLUSION

The microburst analyzed in this report lasted for approximately 22 minutes (Table IX-1). Its radial velocity differential exceeded 20 m/s for over 8 minutes. At the time of peak velocity, the diameter of the outflow was less than 4 km. During this time the size and intensity of the wind shear would represent the greatest hazard to an arriving or departing aircraft. The distance across the maximum velocity change had expanded to 10 km prior to cell dissipation (Table IX-1). This study documented the persistence and strength of precursors such as rotation, divergence, convergence and a descending core. The reliable detection of these features by the microburst algorithm provided a timely warning of the wind shear before it attained an operationally hazardous level. In particular, an algorithm keying on upper-level features declared the wind shear while the surface divergence was less than 10 m/s. This would have provided 18 minutes lead time prior to the maximum outflow strength

Microburst case-studies are pertinent to the development and enhancement of the TDWR microburst detection algorithm. It is important to be able to track the altitude of the reflectivity maxima with time. Based on this analysis, a descending reflectivity core appears to provide the best evidence of the microbursts occurrence. The strengthening of divergent storm tops is a precursor to the maximum outflow intensity. Another precursor to the 24 August 1986 microburst was the combination of rotation and reflectivity notching at mid-levels. An enhancement to the rotation feature extraction algorithm would be to detect reflectivity structures such as notches. If both features are present there might be a greater likelihood of a wind shear.

TABLE IX-1. Microburst Outflow Time History

Time UT	Radial Velocity Difference (m/s)	Diameter km	Range km	Azimuth deg
190129	8	2.6	26	294
190532	9	3.7	25	292
191049	12	3.7	22	291
191525	18	3.7	22	280
191932	24	3.5	21	283
192042	24	3.7	21	283
192128	22	4.9	22	281
192215	21	5.7	22	280
192349	24	6.8	22	279
192459	21	7.5	22	279
192546	21	7.6	22	277
192632	21	8.8	22	278
192806	18	9.0	22	274
193045	15	10.1	21	274
193217	12	10.0	19	271

REFERENCES

Burrows, D.A. and L.F. Osborne, 1986: Precipitation Loading in Wet Microbursts. 23RD CONFERENCE ON RADAR METEOROLOGY, Snowmass, Colorado. 97-100.

Campbell, S.D., 1986: Microburst Recognition: An Expert System Approach, 23RD CONFERENCE ON RADAR METEOROLOGY, Snowmass, Colorado. 26-29.

Campbell, S.D., 1988: Microburst Precursor Recognition Using An Expert System Approach. FOURTH INTERNATIONAL CONFERENCE ON INTERACTIVE INFORMATION AND PROCESSING SYSTEMS FOR METEOROLOGY, OCEANOGRAPHY, AND HYDROLOGY. Anaheim, California.

Campbell S.D., and M.W. Merritt, 1987: Microburst Detection Algorithm. PROJECT REPORT ATC-145.

Caracena, F., J. McCarthy, and J.A. Flueck, 1983: Forecasting the likelihood of microbursts along the Front Range of Colorado. 13TH CONFERENCE ON SEVERE LOCAL STORMS. American Meteorological Society, Boston. 261-264.

Caracena, F., R. Ortiz, and J.A. Augustine, 1986: The Crash of Delta Flight 191 at Dallas-Fort Worth International Airport on 2 August 1985: Multiscale Analysis of Weather Conditions. NOAA TECHNICAL REPORT ERL 430-ESG 2. U.S. Govt. Printing Office, Washington, DC. 1-33.

Clark, D.A., 1988: Observability of Microbursts with Doppler Weather Radar During 1986 in Huntsville, Alabama. PROJECT REPORT ATC-160.

Crocker,S.C., 1988: TDWR PRF Selection Criteria. Project Report ATC-147.

DiStefano, J.T., 1987: Study of Microburst Detection Performance During 1985 in Memphis, Tennessee. PROJECT REPORT ATC-142.

Eilts, M.D., 1987: Nowcasting low-altitude wind shear with a Doppler radar. AIAA 25TH AEROSPACE SCIENCES MEETING, Reno, Nevada. 1-5.

Eilts, M.D., and R.J. Doviak, 1987: Oklahoma Downbursts and Their Asymmetry. JOUR. OF CLI. AND APPL. METEOR., 26. 69-78.

Eilts, M.D., 1988: Use of a Single Doppler Radar to Estimate the Runway Wind Shear Component in Microburst Outflows. AIAA 26TH AEROSPACE SCIENCES MEETING, Reno, Nevada. 1-5.

Elmore, K.L., 1986: Evolution of a Microburst and Bow-Shaped Echo during JAWS. 23RD CONFERENCE ON RADAR METEOROLOGY, Snowmass, Colorado. 101-104.

Evans, J.E., 1983: Ground Clutter Cancellation for the NEXRAD System. Project Report ATC-122.

Evans, J.E., and D. Johnson, 1984: The FAA transportable Doppler weather radar. 22ND CONFERENCE ON RADAR METEOROLOGY, Zurich, Switzerland. 246-250.

Fujita, T.T. 1981: Tornadoes and Downbursts in the Context of Generalized Planetary Scale. J. ATMOS. SCI., 38. 1512-1534.

Fujita, T.T., and R.M. Wakimoto, 1981: Five Scales of Airflow Associated with a Series of Downbursts on 16 July 1980. MON. WEA. REV., 109. 1438-1456.

Fujita, T.T., 1986: DFW Microburst. SMRP RESEARCH PAPER # 217, University of Chicago. 1-154.

Fujita, T.T., 1987: Monrovia Microburst of 20 July 1986: A Study of "SST". SMRP RESEARCH PAPER # 219, University of Chicago. 1-4.

Hjelmfelt, M.R., 1984: Radar and Surface Data Analysis of a Microburst in JAWS. 22ND CONFERENCE ON RADAR METEOROLOGY, Zurich, Switzerland. 64-69.

Hjelmfelt, M.R., and R.D. Roberts, 1985: Microburst Lines. 14TH CONFERENCE ON SEVERE LOCAL STORMS, Indianapolis, Indiana. 297-300.

Hjelmfelt, M.R., and R.D. Roberts, 1986: Observational and Numerical Study of a Microburst Line-Producing Storm. 23RD CONFERENCE ON RADAR METEOROLOGY, Snowmass, Colorado. 77-80.

Hjelmfelt, M.R., 1987: Structure and Life Cycle of Microburst Outflows Observed in Colorado. JOUR. OF CLI. AND APPL. METEOR., 27. 900-927.

Isaminger, M.A., 1987: A Preliminary Analysis of Huntsville Microburst Precursors. PROJECT REPORT ATC-153.

Kessinger, C.J., M.R. Hjelmfelt, and J.W. Wilson, 1983: Low-level microburst wind structure using Doppler radar and PAM data. 21ST CONFERENCE ON RADAR METEOROLOGY, Edmonton, Alberta. 609-615.

Kessinger, C.J., R.D. Roberts, and K.L. Elmore, 1986: A Summary of Microburst Characteristics from Low-Reflectivity Storms. 23RD CONFERENCE ON RADAR METEOROLOGY, Snowmass, Colorado. 105-108.

Mann, D.R., 1988: TDWR Clutter Residue Map Generation and Usage. Project Report ATC-148.

McCarthy, J., J.W. Wilson, and T.T. Fujita, 1982: The Joint Airport Weather Studies Project. BULL. AMER. METEOR. SOC., 63. 15-22.

McCarthy, J. and J.W. Wilson, 1984: The Microburst as a Hazard to Aviation: Structure, Mechanisms, Climatology, and Nowcasting. PROCEEDINGS, NOWCASTING II SYMPOSIUM, Noorkoping, Sweden. 21-30.

McCarthy, J., J.W. Wilson, and M.R. Hjelmfelt, 1986: Operational Wind Shear Detection and Warning: The CLAWS Experience at Denver and Future Objectives. 23RD CONFERENCE ON RADAR METEOROLOGY, Snowmass, Colorado. 18-21.

McCarthy, J., and P. Clyne, 1987: A Strategy For Avoidance of Hazardous Convective Weather in the Airport Terminal Area. 40TH INTERNATIONAL AIR SAFETY SEMINAR, Tokyo, Japan. 1-32.

Merritt, M.W., 1987: Automated Detection of Microburst Wind Shear for Terminal Doppler Weather Radar. DIGITAL IMAGE PROCESSING AND VISUAL COMMUNICATIONS TECHNOLOGIES IN METEOROLOGY. Cambridge, Massachusetts.

National Research Council, 1983: LOW-ALTITUDE WIND SHEAR AND ITS HAZARD TO AVIATION. National Academy Press, Washington, D.C., 166 pp.

NEXRAD Program Office, 1985: Divergence Detection Algorithm Description. NX-DR-03-042/10, NEXT GENERATION WEATHER RADAR ALGORITHM REPORT.

Rinehart, R.E. and M.A. Isaminger, 1986: Radar Characteristics Of Microbursts in the Mid-South. 23RD CONFERENCE ON RADAR METEOROLOGY, Snowmass, Colorado. 116-119.

Rinehart, R.E., J.T. DiStefano, and M.M. Wolfson, 1987: Preliminary Memphis FAA/Lincoln Laboratory Operational Weather Studies Results. PROJECT REPORT ATC-141.

Roberts, R.D. and J.W. Wilson, 1984: Precipitation and Kinematic Structure of Microburst-Producing Storms. 22ND CONFERENCE ON RADAR METEOROLOGY, Zurich, Switzerland. 71-76.

Roberts, R.D. and J.W. Wilson, 1986: Nowcasting Microburst Events Using Single Doppler Radar. 23RD CONFERENCE ON RADAR METEOROLOGY, Snowmass, Colorado. 14-17.

Wakimoto, R.M., 1985: Forecasting Dry Microburst Activity over the High Plains. MON. WEA. REV., 113. 1131-1143.

Wakimoto, R.M., and V.N. Bringi, 1988: Dual-Polarization Observations of Microbursts Associated with Intense Convection: The 20 July Storm during the MIST Project. MON. WEA. REV. 116, 1521-1539.

Wilson, J.W., and D. Reum, 1986: The Hail Spike: Reflectivity and Velocity Signature. 23RD CONFERENCE ON RADAR METEOROLOGY, Snowmass, Colorado. 62-65.

Wilson, J.W., R.D. Roberts, C.J. Kessinger, and J. McCarthy, 1984: Microburst Wind Structure and Evaluation of Doppler Radar for Airport Wind Shear Detection. JOUR. OF CLI. AND APPL. METEOR., 23. 898-914.

Witt, A., and S.P. Nelson, 1984: The Relationship Between Upper-Level Divergent Outflow Magnitude As Measured By Doppler Radar And Hailstorm Intensity. 22ND CONFERENCE ON RADAR METEOROLOGY, Zurich, Switzerland. 108-111.

Wolfson, M.M., 1983: Doppler Radar Observations of an Oklahoma Downburst. 21ST CONFERENCE ON RADAR METEOROLOGY, Edmonton, Alberta. 590-595.

Wolfson, M.M., 1988: Characteristics of Microbursts in the Continental United States. LINCOLN LABORATORY JOURNAL, 1. 49-73.

Zrnic, D.S., 1987: Three-body scattering produces precipitation signature of special diagnostic value. RADIO SCIENCE, 22. 76-86.